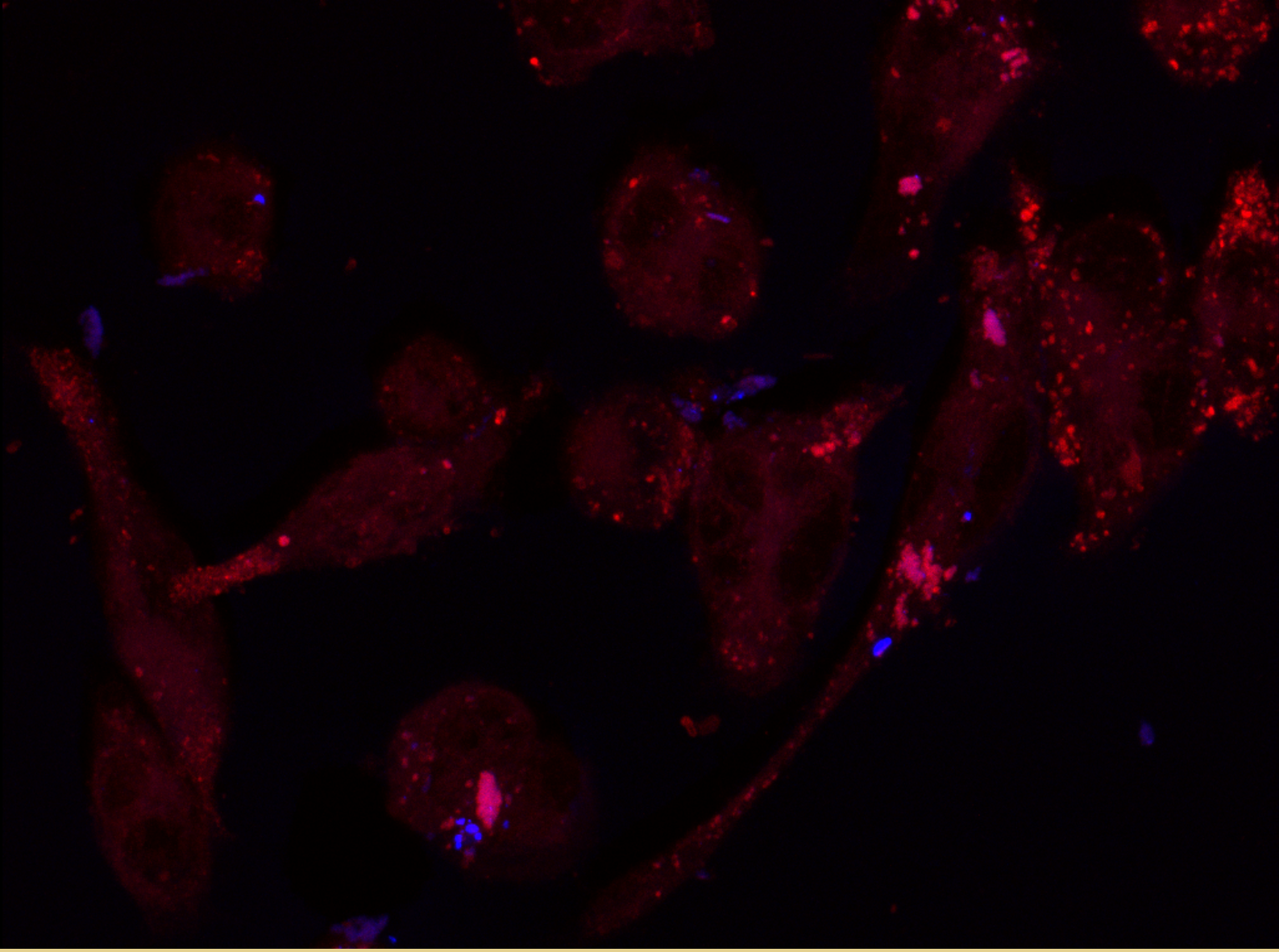

Daniela Neves Antunes

Immunomodulatory effect of different components of the cell wall of *Alternaria spp.*

Dissertação de Mestrado em Bioquímica

Julho 2017

· U C ·

Universidade de Coimbra

Immunomodulatory effect of different components of the cell wall of *Alternaria spp.*

Daniela Neves Antunes

UNIVERSIDADE DE COIMBRA

2017

Dissertação apresentada ao Departamento de Ciências da Vida da Universidade de Coimbra para obtenção do Grau de Mestre em Bioquímica, realizada sob a orientação científica da Professora Doutora Teresa Maria Fonseca Oliveira Gonçalves (Universidade de Coimbra) e da Professora Doutora Paula Cristina Veríssimo Pires (Universidade de Coimbra).

Funding: This work was supported by FEDER funds through the Operational Programme Competitiveness Factors - COMPETE and national funds by FCT under the strategic project UID / NEU / 04539 / 2013; and also HealthyAging2020:CENTRO-01-0145-FEDER-000012 of Centro2020 and Portugal2020, European Union Funds (FEDER and COMPETE)

Acknowledgements

"Só os anjos saberão
Quantos mundos ainda vou viver
Quantas páginas vou escrever"

Firstly, I would like to acknowledge all the support of my advisor, Professor Teresa Gonçalves and for inspiring me through my path.

I also want to thank all my colleagues on the laboratory, for earring my thoughts out loud, my struggles, and helping in whatever I needed. You deserve a cake, at least.

I want to show my gratitude to all my close friends, Lara and all "Fófócas" for being by my side since the beginning, Pedro & Fábio, Andrea, and Sara, in other words, everyone that inspire me and that I inspired in my path. I have created so many life's stories. With you everything became easier to do and to accomplish. I know I can count on you like… 1,2,3… and you will be there.

Finally, I must express my very profound gratitude to my family, they have been my rock, giving me unfailing support and unceasing encouragement. Mostly, I want to show my gratitude to my parents and my sisters, who since I was a little girl helped me to dream higher, to believe in me.

To family and friends,

Because it is all about love,

The sincerest,
Thank You.

Index

List of tables vii
List of figures ix
List of abbreviations xi
Chapter 1 1
1. Introduction 3
1.1 Fungi 3
1.1.1 Fungal cell wall 4
1.1.2 Hyphal growth 5
1.1.1.1 Melanin *7*
1.1.1.2 Chitin *8*
1.1.1.3 β-glucan *9*
1.2 *Alternaria* 10
1.2.1 Genus *Alternaria* 10
1.2.1.1 Alternaria biological traits *10*
1.2.2 *Alternaria infectoria* 11
1.3 Fungal infections and the immune innate system 11
1.3.1 Interaction between macrophages and fungi 12
1.3.1.1 Pattern-recognition receptors (PRRs) *12*
1.3.1.2 Fungal pathogen-associated molecular patterns (PAMPs) *13*
1.3.2 Macrophages immune response to fungal infections 13
1.4 Aims 16
Chapter 2 17
2.Materials and Methods 19
2.1 Fungal Strains 19
2.1.1. Fungal Culture media and Solutions 19
2.1.1. Fungal Growth Conditions 19
2.1.3. Quantification of chitin and β-(1,3)-glucan content on the cell wall of *A. infectoria* treated with nikkomycin 20
2.1.3. *A. infectoria* harvest 20
2.2. Preparation of nanoparticles of the cell wall of *A. infectoria* 20
2.2.1. *A. infectoria* cell wall isolation and nanoparticles preparation 20
2.2.2. Flow Cytometry of CWNPs 21
2.2.3. Zeta potential of CWNPs 21
2.2.4. Transmission electron microscopy (TEM) to analyse the CWNPs 22

2.3 Macrophages-NPs interaction assays 22
2.3.1 Macrophages Cell Line 22
2.3.2. Cell culture 22
2.3.3 Interaction of *A. infectoria* CWNPs with macrophages 23
2.3.4. Transmission Electron Microscopy (TEM) assay 23
2.3.5. Fluorescence microscopy assay 24
2.3.6. Viability test 24
2.3.7. Fluorescence Microscopy assay for chitin of the CWNPs and macrophages acidic organelles 25
2.3.8. Relative quantification of TNF-alpha gene (Tumor necrosis factor alpha gene) expression in macrophages 25
2.4. Statistical Analysis 27
Chapter 3 29
3. Results 31
3.1. Nanoparticles characterization 31
3.2.1. Differential Fungal Growth 31
3.1.2. Chitin and β-(1,3)-glucan content on *A. infectoria* cell wall grown with nikkomycin 31
3.1.3. Flow Cytometry characterization of nanoparticles prepared from the fungal cell wall of *A. infectoria* - CWNPs 32
3.1.4. Zeta potential and size of the CWNPs 33
3.1.5. Analysis of the CWNPs morphology by TEM 35
3.2. Interaction assays 36
3.2.1. TEM study on the interaction of ctCWNPs with macrophages 36
3.2.2. Fluorescent microscopy assay for Sialic Acid and Deoxyribonucleic acid 37
3.2.4. Macrophages viability upon exposure to CWNPs 38
3.2.5. Internalization of CWNPs of *A. infectoria* and acidic organelles 40
3.2.5.1. Characterization of the dynamics of CWNPs when interacting with macrophages 42
3.2.5.2. 3D analysis 44
3.2.6. Relative quantification of Tumor necrosis factor alpha gene (TNF-α) expression in macrophages during interaction with CWNPs 45
Chapter 4 47
4. Discussion 49
4.1 Nanoparticles characterization 49
4.2 Macrophages-CWNPs interaction characterization 51
Chapter 5 55

5. Final Conclusions _____ **57**
Chapter 6 _____ **59**
6. Future Perspectives _____ **61**
Chapter 7 _____ **63**
7. Bibliographic References _____ **65**

List of tables

Table 1 Oligonucleotides sequences used in quantitative Real Time PCR 26
Table 2 Quantitative Real Time PCR parameters for amplification 27
Table 3 Nanoparticles' size distribution and zeta potential analysed using the Beckman Coulter® DelsaTM Nano C Particle Analyser instrument 34
Table 4 Nanoparticles diameter (nm) measured with FEI-Tecnai G2 Spirit Bio Twin transmission electron microscope at 100 kV 36

List of figures

Figure 1 : Diagram showing the putative organization of polymers on fungal cell wall 4
Figure 2: Transport of MMD-CHS- bound vesicles to the growth region and lateral cell wall 6
Figure 3: Macrophage-fungus interaction 15
Figure 4: Growth of *A. infectoria* mycelia with different compounds 31
Figure 5: Modulation of cell wall components by nikkomycin 32
Figure 6: Flow cytometry signatures of the CWNPs 33
Figure 7: TEM images of CWNPs of *A. infectoria* 35
Figure 8: TEM observations of macrophages RAW 264.7 36
Figure 9: Macrophages morphology upon exposure to *A. infectoria* CWNPs 38
Figure 10: Macrophage viability during interaction with CWNPs 39
Figure 11: Intracellular distribution of CWNPs *A. infectoria* in RAW 264.7 macrophages and acidic compartments 40
Figure 12: Analysis of area and number of CWNPs internalized by RAW 264.7 42
Figure 13: Average number of macrophages that internalized CWNPs per time 43
Figure 14: 3D projections of *A. infectoria* CWNPs, in RAW 264.7 macrophages 44
Figure 15: Relative quantification of Tumor necrosis factor alpha gene (TNF-α) expression in macrophages after 1 h and 3 h interaction with ctCWNPs and pyrCWNPs, caspCWNPs or nkCWNPs 46

List of abbreviations

3D – three-dimensional

CWNPS - *A. infectoria* cell walls nanoparticles (CellWall NanoParticles)

ctCWNPS - *A. infectoria* cell walls nanoparticles grown under control conditions

caspCWNPS - *A. infectoria* cell walls nanoparticles grown with caspofungin

nkCWNPS - *A. infectoria* cell walls nanoparticles grown with nikkomycin

pyrCWNPS - *A. infectoria* cell walls nanoparticles grown with pyroquilon

CWF - CalcoFluor White

AIDS – Acquired Immunodeficiency Syndrome

AMP – Antimicrobial Peptides

CHS – Chitin Synthases

CLRs – C-type Lectin Receptor

DAKO – Dakocytomation fluorescent mounting medium

DAPI – 4',6-diamidino-2-phenylindole dihydrochrolide

DHN – 1,8 dihydroxynaphthalene

DLS – Dynamic Light Scattering

DMEM – Dulbecco's Modified Eagle's Medium

FBS – Fetal Bovine Serum

FITC – Fluorescein

FSC – Forward-Scattered light

iNOS – inducible Nitric Oxide Synthase

ITAM - Immunoreceptor Tyrosine-based Activation Motif

L-DOPA – L-3,4-dihydroxyphenelalanine

MMD – Myosin Motor Domain

Myd88 - myeloid differentiation primary response protein 88

NADPH - Nicotinamide Adenine Dinucleotide Phosphate

PAMP – Pathogen-Associated Molecular Patterns

PBS – Phosphate Buffered Saline solution

PDA – Potato Dextrose Agar

PDI – Polydispersity index

PRR – Pattern Recognition Receptors

RT-qPCR – Quantitative Reverse Transcription PCR

ROI – Reactive Oxygen Intermediates

ROS – Reactive Oxygen Species

SD – Standart Deviation

SEM – Standart Error of the Mean

SPK – Spitzenkörper

SSC – Side-Scattered light

TEM – Transmission Electron Microscopy

TLRs – Toll-Like Receptors

TNF-α - Tumor Necrosis Factor alpha

TNF-alpha gene – Tumor Necrosis Factor alpha gene

UV – Ultraviolet Light

WGA - Wheat Germ Agglutinin

YME – Yeast-Malt Extract

Abstract

Fungi are ubiquitous in our environment and a healthy innate immune system is essential to maintain adequate protection from fungal infections and sensitization. Most human host-fungal interactions at the body surfaces are non-infectious although opportunistic fungi can cause severe pathologies in susceptible individuals. The fungal cell wall is located outside the cell membrane, this way, the diseases caused by fungi are very likely associated with the interaction of components on the cell with the host cells. Fungal cell wall has an important role for fungal survival, however it is a dynamic structure, that adapts to different environments, also helping fungus to escape from the immune system. As such, both the knowledge of how fungal cell wall modulates their components on different environment, and the understanding of the mechanisms of interaction between the fungi and innate immune system, are important to develop more effective future antifungal strategies.

This work had as main goal the characterization the immunomudolatory effect of different components of the cell wall of *Alternaria infectoria*, as a model organism of a filamentous fungi that is an opportunistic agent. It was developed a model of *in vitro* interaction of mice macrophages (RAW 264.7 cell line) with nanoparticles obtained from *A. infectoria* mycelial fungal cell walls (Cell Wall NanoParticles - CWNPs). The cell wall was modulated using inhibitors of fungal cell wall components: an inhibitor of β-(1,3)-glucan synthesis, caspofungin; an inhibitor of chitin synthases, nikkomycin Z; and an inhibitor of DHN-melanin synthesis, pyroquilon. The CWNPs characterization was accomplish through flow cytometry, nanoparticles size distribution and zeta potential analysis, and by transmission electron microscopy (TEM). The interaction of the CWNPs with the macrophages was analysed using TEM and fluorescence microscopy; macrophages viability was assessed by the trypan blue staining test; and with the quantification of the relative expression of the gene that codes TNF-alpha gene through quantitative reverse transcription PCR (RT-qPCR).

The obtained CWNPs proved to be a good model of interaction of macrophages with filamentous fungal cell walls. The results obtained showed that DHN-melanin inhibition by pyroquilon, enhance a higher macrophage activation than control CWNPs. The CWNPs prepared from fungus where the modulation of β-(1,3)-glucan was achieved with caspofungin, triggered a macrophage activation, with a 6-fold (1 h exposure) or 3-fold (3 h exposure) increase of TNF-alpha gene expression. Moreover, the increase of chitin and melanin cell wall content, by nikkomycin Z, resulted in a delayed activation of macrophages.

This work demonstrates the usefulness of a model of filamentous fungi cell wall nanoparticles that allows a correct evaluation of the interaction of filamentous fungi with host cells. It also proves that the modulation of chitin and melanin, besides β-glucan, is an important strategy to control the stimulation of cells of the innate immune system.

Keywords: *Alternaria infectoria*; cell wall; nanoparticles; chitin; nikkomycin; β-(1,3)-glucan; caspofungin; melanin; pyroquilon; innate immune response; macrophages

Resumo

Os fungos são organismos onipresentes no nosso ambiente, e um sistema imune inato competente é essencial para manter uma proteção adequada contra infeções fúngicas e sensibilização a fungos. A maioria das interações fúngicas com o Homem não são infeciosas. No entanto, os fungos oportunistas podem causar patologias graves em indivíduos mais suscetíveis. A parede celular fúngica, por estar localizada mais externamente, está associada às doenças causadas por fungos resultantes da interação entre componentes da parede celular e as células hospedeiras. A parede celular, que tem um papel importante para a sobrevivência de fungos, é uma estrutura dinâmica que se adapta a diferentes ambientes, podendo ajudar o fungo a escapar do sistema imunológico. Assim, o conhecimento acerca da parede celular fúngica e da modulação do conteúdo dos seus componentes em diferentes ambientes e a compreensão dos mecanismos de interação entre os fungos e o sistema imunitário inato, são pontos importantes para desenvolvimento de futuras estratégias antifúngicas mais efetivas.

O objetivo principal deste trabalho centrou-se na caracterização do efeito imunomodulador de diferentes componentes da parede celular de *Alternaria infectoria*, como organismo modelo de um fungo filamentoso e de agente oportunista. Foi desenvolvido um modelo de interação *in vitro* entre macrófagos murinos (linha celular RAW 264.7) com nanopartículas obtidas a partir de paredes celulares fúngicas do micélio de *A. infectoria* (*Cell Wall NanoParticles* - CWNPs). A parede celular fúngica foi modulada usando inibidores dos seus componentes: um inibidor da síntese de β-(1,3)-glucano, a caspofungina, um inibidor de enzimas responsáveis pela síntese de quitina, a nicomicina Z, e um inibidor da síntese de DHN-melanina, o piroquilon. A caracterização das CWNPs foi realizada através de citometria de fluxo, pela distribuição de tamanho das nanopartículas e análise de potencial zeta e ainda por microscopia eletrónica de transmissão (TEM). A interação das CWNPs com os macrófagos foi analisada recorrendo a TEM e microscopia de fluorescência. A análise da viabilidade dos macrófagos foi realizada pelo teste de coloração com azul de tripano, enquanto a quantificação da expressão relativa do gene que codifica para o TNF-alpha foi obtida por RT-qPCR (*quantitative reverse transcription PCR*).

As CWNPs obtidas provaram ser um bom modelo de interação de macrófagos com paredes celulares de fungos filamentosos. Os resultados obtidos mostraram que a inibição de DHN-melanina por piroquilon, provoca uma maior ativação de macrófagos do que CWNPs controlo. As CWNPs preparadas a partir de fungos onde a modulação de β-(1,3)-glucano foi alcançada com caspofungina, desencadearam uma ativação dos macrófagos com um aumento de 6 vezes (1 h de exposição) ou 3 vezes (3 h de

exposição) da expressão do gene TNF-alfa. Além disso, o aumento do conteúdo em quitina e melanina da parede celular, modulado por nicomicina Z, resultou numa ativação tardia dos macrófagos.

Este trabalho demonstra a utilidade de um modelo de nanopartículas obtidas a partir de paredes de fungos filamentosos, que permite uma avaliação correta da interação destes fungos com células do hospedeiro. Também prova que a modulação de quitina e de melanina, para além do β-glucano, é uma estratégia importante para o controlo da estimulação de células do sistema imune inato.

Palavras-chave: *Alternaria infectoria*; parede celular; nanoparticulas; quitina; nicomicina; β-(1,3)-glucano; caspofungina; melanina; pyroquilon; resposta do sistema imunitário; macrófagos

Chapter 1

Introduction

1. Introduction

In the last decades, fungal infections are considered an emergent human health problem, due to the increase of number of immunosuppressed individuals. Also, it has been recognized the importance of fungi in the onset of severe respiratory diseases, due to fungal sensitization, in people exposed to fungal particles, spores or parts of mycelial hyphae (Denning *et al*., 2014) a great part belonging to the genus *Alternaria*. The diseases caused by fungi are very likely associated with the interaction of components on the fungal cell surface with the host cells.

To introduce this work, it will be given an overview of the scientific literature regarding fungi, in particular *Alternaria infectoria*. Secondly, it will be described how the innate immune system respond to a fungal infection. In particular, how the fungal recognition and interaction by the host innate immune cells is achieved and proceed.

1.1 Fungi

Fungi can be found throughout the World and have been estimated to be approximately 25% of the global biomass (Edward, 2009). Fungi have a huge impact on our daily lives. Although unicellular yeasts are used mainly for the production of alcoholic beverages and bread, filamentous fungi have many other uses (Rokern, 2007). They may live as saprophytes, parasites or symbionts of animals and plants in indoor as well as outdoor environments, and are associated with a wide spectrum of diseases in humans. Fungi are heterotrophic eukaryotes that are traditionally and morphologically classified into yeast and filamentous forms. Some can exist in different forms and reversibly switch from one to the other in response to stimuli such as those observed during infections. Humans are widely exposed to fungi by inhaling or ingesting spores or small yeast cells that can establish symbiotic, commensal, latent or pathogenic relationships. Additionally, their ability to colonize different niches in the human body involves specific reprogramming events that allows them to adapt to environmental conditions, fight for nutrients and support stresses generated by host defence mechanisms (Woudenberg *et al*., 2015).

The clinical relevance of fungal diseases has increased in the second half of the twentieth century, mostly caused by the increase of immunosuppressed individuals (due to the increased prevalence of cancer, chemotherapy, organ transplantation, autoimmune diseases and acquired immunodeficiency syndrome - AIDS) (Romani, 2004).

In contrast to pollen, fungi may not only cause type I allergic reactions, but also a large number of other illnesses, including allergic bronchopulmonary mycosis, allergic sinusitis, hypersensitivity pneumonitis, and atopic dermatitis and are frequently linked with severe allergic asthma (sensitization reported in up to 80% of asthmatic patients) (Simon-Nobbe *et al.*, 2008).

The crude mortality from opportunistic fungal infections still exceeds 50% in most human studies, and has been reported to be as high as 95% in bone-marrow transplant recipients infected with *Aspergillus fumigatus*. Since fungal pathogens are eukaryotes, they share many biological processes with humans, consequently many antifungal drugs are highly toxic to humans when used therapeutically (Romani, 2004).

1.1.1 Fungal cell wall

Among eukaryotes, cell walls are found in many plants, fungal and algal species. The fungal cell wall is located outside the cell membrane and provides both protective and aggressive functions. It is protective because it acts as an initial barrier that contacts with hostile environments encountered by the fungus. Also has an aggressive function due to the harbour of hydrolytic and toxic molecules, most of them moving in the cell wall and are required by the fungi to invade the host and resist against host defence mechanism (Casadevall *et al.*, 2009; Latgé, 2007).

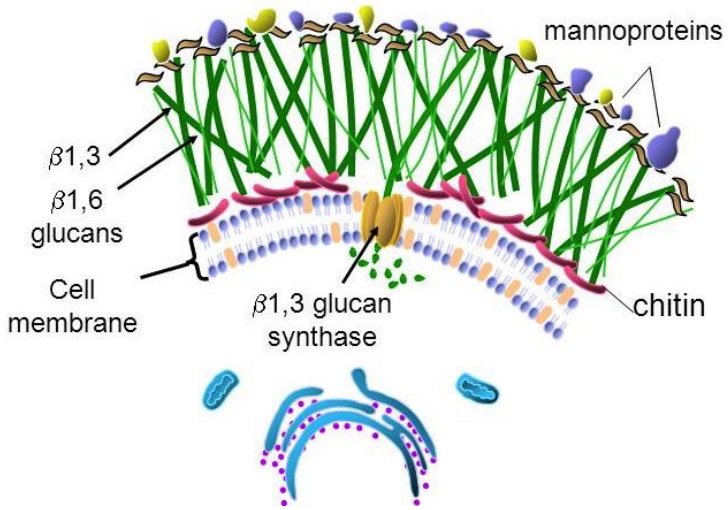

Figure 1 – Diagram showing the putative organization of polymers on fungal cell wall (Adapted from Kartsonis *et al.*, 2003)

The composition and structural organization of the cell wall is not set immutably and is constantly reshuffled (Casadevall *et al.*, 2009) . Fungal cell wall is composed of a tight, semipermeable fibrillar network of polymers such as glucans, chitin,

mannans and/or galactomannan, and glycoproteins (Lipke & Ovalle, 1998). Polysaccharides account for more than 90% of fungal cell wall (Latgé, 2007).

The cell wall of most fungi remains insufficiently studied and its biosynthesis incompletely understood, especially on filamentous fungi, consequence of the technically impossibility of analysing the cell wall polymer without an enzymatic and physicochemical treatment. Likewise, the current methodologies do not provide good insights about the distribution and localization of specific polysaccharides since they may destroy the three-dimensional (3D) polysaccharide network of fungal cell wall (Latgé, 2007).

In most fungi, the fungal cell wall has several constituents (Figure 1), including chitin, β-(1,3)-glucan, β-(1,6)-glucan, mannosylated proteins and phospolipomannan, where β-(1,3)-, (1,6)-glucans are linked to chitin via a β-(1,4)-linkage (Latgé, 2007). This glucan-chitin complex is covalently bound to other polysaccharides, the composition of which varies specifically with the pathogen. Moreover, β-(1,6)-glucosidic linkages account for 3% of the total glucan linkages in *Saccharomyces cerevisae* and *Aspergillus fumigatus*, respectively (Latgé, 2007). Furthermore, conidia cell wall of *A. fumigatus* is covered by hydrophobins and melanin, in contrast with the exposure of β-(1,3)-glucans, galactomannan, galactosaminagalactan and N-glycosylated proteins on the surface of germinating conidia, a further evidence the high variability of the fungal cell wall. Nevertheless, major differences have also been noticed among fungal morphotypes in the same species. Many studies using fluorescent markers or radiolabelled precursors suggest that septa and apices have different structures to the lateral, older cell wall regions (Latgé, 2007).

The fungal cell wall is a dynamic structure, continuously evolving in response to the environment and during cell cycle and somatic growth. The panel of diseases caused by fungi are very likely associated with components on the cell wall. Overall, the cell wall is an attractive target to the development of novel tools to clear or prevent deleterious effects for the host during infections.

1.1.2 Hyphal growth

The basic unit of growth of filamentous fungi is the hypha, a long cylinder with a slightly tapered apex.

Genetic analyses have identified many genes that participate in hyphal morphogenesis. However, in *Candida albicans* hyphal morphology can be regulated independently of the expression of hyphal genes (Naseem *et al*., 2015). Furthermore, the shape of the hypha is determined by cell wall assembly. In cells that do have a wall (most bacteria, algae, fungi and plants) an internal hydrostatic balance provides both

mechanical support for free-standing structures and a force that drives cellular expansion, substrate penetration and other processes. Therefore, during cell growth (expansion and division), remodelling of the cell wall is required to increase the cellular volume. Additionally, cell wall-loosening enzymes, such as chitinases and glucanases, participate in the breakage of polysaccharide chains, such as chitin and β-(1,3)-glucans, allowing the addition of newly arrived material and generating free ends, substrate for cross-linking enzymes, that rigidify the cell wall (Riquelme, 2013).

The mechanism underlying the growth of fungal hyphae are rooted in the physical property of cell pressure. Calcium gradients regulate tip growth, and secretory vesicles that contribute to this process are actively transported to the growing tip by molecular motor that move along cytoskeletal structures, which kinesin-1, kinesin-3 and myosin-V cooperate in polarized growth (Enjalbert *et al.*, 2006).

Polarized growth (that allows the asymmetric transport) as tip growth occurs in fungal hyphae, neurons, root hairs, and pollen tubes. But among these cell types, only fungal hyphae can potentially extend indefinitely under certain conditions (Riquelme, 2013). The polar transportation takes vesicles to an ultrastructure present in the tip of an actively growing hyphae or under morphogenesis, the Spitzenkorper (SPK), trough filamentous actin and microtubules in the cytoskeleton (Fernandes, Gow & Gonçalves, 2016).

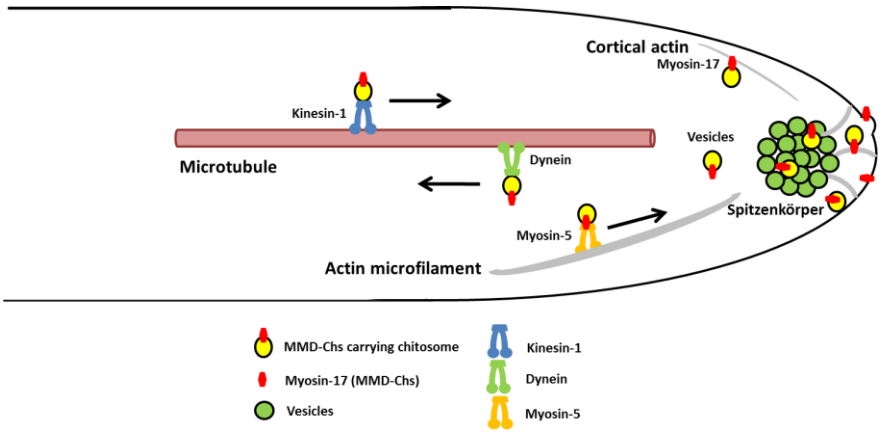

Figure 2: Transport of MMD-CHS- bound vesicles to the growth region and lateral cell wall. With the fusion with the plasma membrane, the enzymes will be insert on it and start the synthesize of the fungal cell wall (Adapetd from Fernandes, Gow & Gonçalves, 2016)

SPK is in the cytoplasm of the extreme apex of the hypha (Figure 2), and contains secretory vesicles and micro-vesicles that will fuse with the plasma membrane. One of SPK function is to help in the cell wall-building process (Riquelme, 2013).

Chitin is an important cell wall component conferring rigidity. Chitin are synthesized by chitin synthases (CHS), which some have and N-terminal myosin motor-

like domains, constituting the MMD-CHS (Myosin Motor Domain – Chitin synthases). The CHS are insert on the membrane of the growing hyphae tip to synthesize chitin for the cell wall. The transportation for the apical growth is made by the MMD-CHS trough chitin filaments (bi-directional motility) or trough along microtubules, which for the anterograde motility is kinesin-1 dependent and for the retrograde is dynein dependent (Fernandes, Gow & Gonçalves, 2016).

Moreover, polarized growth in fungi is considered a virulent factor and the yeast-to-hypha transition or the differentiation of special invasion structures at the hypha tip of filamentous fungi are considered to play an important role in adhesion and invasion of surfaces and plant or animal hosts (Brand, 2012). The deletion of the CHS either abolishes phyto-pathogenicity or dramatically decreases the virulence (fungi quickly recognized), such as the ones with MMD domains, which retain the filamentous fungi ability to invade the host (Treitschke *et al*., 2010).

In this way, hyphal growth in filamentous fungi is a relevant matter to apply research efforts, due to its importance in the pathogenicity but also because it constitutes a target to explore for novel strategies to control fungal diseases.

1.1.1.1 Melanin

One of the compounds on fungal cell wall is melanin, usually a black or brown pigment, which are located on the outer layer and is covered by a rodlet layer that confers hydrophobic properties. Melanins are hydrophobic pigments of high molecular weight, negatively charged and are formed by the oxidative polymerization of phenolic and/or indolic compounds. More, this pigment is maintained on reduced state to keep their reductive role.

In fungi, there are three types of melanin, synthesized from an endogenous substrate *via* 1,8-dihydroxynaphthalene (DHN) intermediate or from L-3,4-dihydroxyphenylalanine (L-DOPA) (Eisenman & Casadevall, 2012; Fernandes *et al*., 2016). There are other melanins called pyomelanins, water-soluble brown pigments, derived from L-tyrosine *via* homogenistic acid (Yabuuchi & Ohyama, 1972).

Melanin of fungal cell walls provides protection against UV (ultraviolet light), and gamma radiation (Nosanchuk & Casadevall, 2006). Besides the protective effect against reactive oxygen species (ROS) (Jacobson, 2000; Langfelder *et al*., 2003) and antifungal drugs (Fernandes *et al*., 2016; Nosanchuk & Casadevall, 2006) melanin also may contribute to the higher survival and competitive abilities of melanised fungi, not only in the environment but, in particular, while infecting the plant or animal host. Further, this pigment protects conidia against proteases and hydrolases' digestion by competitive

mechanisms or even against bactericidal and fungicidal proteins (Pombeiro-Sponchiado, 2017).

Moreover, it was reported the importance of melanin pigments on the surface of the *A. fumigatus* conidia to mask components that decrease the cytokine response induced by pathogen-associated molecular patterns (PAMPs) (Latgé, 2010) and the effect of DHN-melanin on phagolysosomes acidification (Thywißen *et al*., 2011). Furthermore, inhibitors of melanin, DHN-melanin, (pyroquilon) proved to synergise with antifungals directed to the synthesis of cell wall components (Fernandes *et al*., 2016) providing its potential as a therapeutic tool.

1.1.1.2 Chitin

Chitin is a polymer of β-(1,4)-linked *N*-acetylglucosamine subunits joined in antiparallel chains hydrogen bonding to produce strong microfibrils. Also, it constitutes an essential part of the fungal cell wall, required for the maintenance of cell integrity.

Furthermore, chitin cross-links to other cell wall polysaccharides and proteins, namely melanin, and form up to 40% of the fungal cell wall. Chitin is synthesized by chitin synthases (CHS), which use UDP-*N*-acetylglucosamine as a substrate to add residues to the growing chain (Eisenman & Casadevall *et al.*, 2012) and in fungi, chitin synthases' genes are grouped into seven classes (Fernandes *et al*., 2014). Besides, the chitin synthases are inactive while transported on plasma, only become activated on membrane, where they are arranged as complexes (Latgé, 2007).

The chitin machinery is different among fungi, however, the multiplicity of CHS domains does not imply redundant roles in cell wall synthesis. Therefore, chitin synthases belonging to classes III, V, VI, and VII are distributed only in the genomes of filamentous fungi and dimorphic yeasts that have high chitin contents in their cell walls, which, class V and VII chitin synthases contain a MMD in their N-terminal region (Fernandes *et al*., 2014, Kong *et al*., 2012). Once this enzymes importance for fitness and virulence of fungal pathogens, they can be regarded as excellent targets for the design of isotype-specific antifungal drugs (Fernandes, Gow & Gonçalves, 2016).

There are two classes of antifungal drugs directed at fungal cell wall components, β-glucan synthase inhibitors, (echinocandins) and chitin synthase inhibitors (nikkomycins and polyoxins). However, fungi can compensate the inhibition with other chitin synthases, in this way, in presence of nikkomycin Z there is an increase of chitin content, once this inhibitor does not inhibit all chitin synthases isoforms. Nevertheless, nikkomycin Z may contribute to a different organization of the chitin microfibrils. And once that the lack of alteration of chitin levels generate a melanin compensation, what leads to

changes in the pattern of melanin deposition (Fernandes *et al.*, 2016; Fernandes *et al.*, 2014).

Additionally, chitin is a PAMP with a size-dependent ability to induce pro- and anti-inflammatory responses via TLR2-dependent and non-TLR receptor systems (Da Silva *et al*., 2009).

1.1.1.3 β-glucan

The formation of the fibrillar core of the cell wall is the branching of β-(1,3)-glucan and cross-linking between β-(1,3)-glucan and chitin and subsequently with the other cell wall polysaccharides (Latgé & Beauvais, 2014).

The fungal cell wall polymer β-(1,3)-glucan is synthesized by the enzyme β-(1,3)-glucan synthase, which is composed with two proteins, the putative catalytic subunit Fks1p, a large-molecular-size polypeptide with 16 transmembrane domains, and the regulatory subunit Rho1p, a small-molecular-size GTPase, which stimulates β-(1,3)-glucan synthase activity in its prenylated form (Anjos *et al*., 2012). Like chitin synthases, only become activated on membrane, and also the number of genes encoding β-(1,3)-glucan synthases and the essentiality of each individual gene vary with the fungal species (Latgé, 2007).

Furthermore, there were identified three families of natural β-(1,3)-glucan synthase inhibitors: the glycolipid papulacandins, which consist of a modified dissaccharide linked to two fatty-acyl chains, acidic terpenoids and cyclic hexapeptides with an N-linked fatty-acyl side-chain (Onishi *et al.*, 2000). In the latter group are the non-competitive inhibitors generally known as echinocandins that are currently the only one of the three families used in clinical practice (Latgé, 2007). The first echinocandin to be used in human health was caspofungin targeting the fungal cell wall synthesis but also important in the regulation of the transcription of gene(s) coding for the β-(1,3)-glucan synthase (Anjos *et al*., 2012).

In addition, caspofungin is fungicidal against some yeasts (most species of *Candida*) but also against some molds (*Aspergillus* but not *Fusarium* and *Alternaria*) and modestly or minimally active against dimorphic fungi (*Blastomyces* and *Histoplasma*).

Nevertheless, the action of echinocandins can be improved due to their synergistic effects when they are combined with polyenes or azoles (Fernandes *et al*., 2016).

Furthermore, this cell wall polysaccharide is recognized by the dectin-1 receptor on the surface of macrophages (Thywißen *et al*., 2011). Dectin-1 induces the production of pro- and anti- inflammatory cytokines and chemokines (Romani, 2004).

1.2 Alternaria

1.2.1 Genus *Alternaria*

Alternaria is a large and complex genus that consists of multiple saprophytic and pathogenic species. Based on phylogenetic and morphological studies, the genus is currently divided into 26 sections (Woudenberg *et al*., 2015). Fungi belonging to the genus *Alternaria* exhibit septated and dark hyphae due to strong wall melanisation. Conidia are large (8-16 x 23-50 µm) and brown, with septations on transverse and longitudinal. The formation of appressorium is essential to form the penetration peg and infect the plant host. Here, melanin works as a barrier to efflux of appressorium solutes (Giraldo & Valent, 2013).

The fungi are mainly known as phytopathogens. However, they are agents of infections in human and animal hosts causing phaeohyphomycoses - opportunistic subcutaneous/invasive infections (Pastor & Guarro, 2008).

Furthermore, *Alternaria* fungi are frequently reported as allergenic, food spoilers and mycotoxicogenic. They also can be found on normal human skin and conjunctiva (Pastor & Guarro, 2008). This fungus has been associated with hypersensitivity pneumotitis, bronchial asthma, and allergic sinusitis and rhinitis, causing also different types of human infections (Denning *et al*., 2014).

Alternaria alternata has been (erroneously) regarded as the most frequent species, followed by *Alternaria tenuissima*, although, the identification of these fungi is quite difficult due to their special sporulation growth conditions, subtle morphological features (Ferrer *et al*., 2003). This difficulty in the classical identification of the genus *Alternaria* has been the reason why numerous cases of alternariosis have been attributed to *A. alternata*. The introduction of advanced identification procedures led to the subsequent attribution ethiology to other species such as *A. infectoria* (Pastor & Guarro, 2008).

1.2.1.1 *Alternaria* biological traits

Genus *Alternaria* have septated and dark hyphae, while conideophores are spetated, of variable length, having sometimes a zigzag appearance. Furthermore, conidia are large (usually 8-16 x 23-50 µm) and brown, has both transverse and longitudinal septations (Larone, 2002). These fungi form appressoria, infection structures essential for penetration into host tissues (at least plant tissues) and leads to the production of germ tubes during germination (Hwang *et al.*,1995)

1.2.2 *Alternaria infectoria*

A. infectoria is a rare opportunistic agent of phaeohyphomycoses. *A. infectoria* is a filamentous fungus that contains melanin in the cell wall and belongs to the group of dematiaceous fungi. The growth is as hyphae, which collectively form the mycelium. In addition, exhibits long, dark conideophores that are produced in strong branched chains owing to the formation of extended septated secondary conidia (spore) between conideophores (Andersen, 1996).

The number of clinical cases of *A. infectoria* infections have increase in last years, mostly due the increasing population of immunocompromised hosts allied to the daily exposure of inhalation *A. infectoria* conidia by humans (the most significant prevalence of fungal particles airborne). One example of a reported case is a 5 years-old boy with a phaeohyphomycoses brain access, caused by *A. infectoria* (Hipolito *et al*., 2009).

Since *A. infectoria* are ubiquitous environmental fungi, occurring in plants, soil, food, and indoor air, they are agents of human allergies and infections, causing phaeohyphomycoses and sometimes progresses to infect the central nervous system. Several epidemiologic studies have reproducibly shown that *Alternaria* sensitization is associated with allergic asthma. Asthma is a chronic inflammatory disease, one of the most common health afflictions worldwide, with approximately 300 million people suffering from it (Murai *et al*., 2012). Nonetheless, the exact mechanism of this association is not totally elucidated.

1.3 Fungal infections and the immune innate system

Humans are constantly exposed to fungi, but only a limited number of fungi cause severe infections, when the host immune system is compromised, a major determinant of which particular forms of disease will develop after exposure to fungi. Therefore, innate immune mechanisms are used by the host to respond to a range of fungal pathogens in a rapid and converse manner. The constructive mechanisms of innate defence are present at sites of continuous interactions with fungi and include the barrier functions of body surfaces and mucosal epithelial surfaces of respiratory, gastrointestinal and genito-urinary tracts (Romani, 2011).

However, most host defence mechanisms are induced after infection. Therefore, their activation requires the recognition of invariant molecular structures shared by large groups of pathogens, the pathogen-associated molecular patterns (PAMPs). In this way, these conditions require that the induced immune response needs to be strong enough to allow pathogen elimination while the host survival is not highjacked. Furthermore, it can prompt this fine-tuned system to establish commensalism or persistency with no excessive proinflammatory pathology.

1.3.1 Interaction between macrophages and fungi

Monocytes, macrophages and neutrophils, as well as some cells that are non-phagocytic (such as epithelial and endothelial cells), mostly contribute to the antifungal innate immune response through phagocytes and direct pathogen killing. Macrophages circulate in tissue, being dispersed through the body, however, some take up in particular tissues, becoming fixed macrophages, while other are motile and are so called free or wandering macrophages.

Host cells express pattern recognition receptors (PRRs), such as toll-like receptors (TLRs), C-type lectin receptors (CLRs) and the galectin family proteins, which sense PAMPs in fungi (Romani, 2011).

1.3.1.1 Pattern-recognition receptors (PRRs)

Against infection the innate immune system is the first line of defence through germ-line-encoded receptors. The PRRs are the receptors able to recognise and initiate an inflammatory response to invading pathogens, which sense conserved chemical signatures called PAMPs. PRRs are best characterised into one of four families: the Toll-like (TLR), NOD-like, RIG-I-like and C-type lectin-like receptors (CLR), each of which differ in ligand recognition, signal transduction and sub-cellular localization (Plato *et al*., 2015).

TLRs are transmembrane (TLR1, TLR2, TLR4, TLR5 and TLR6) or intracellular (TLR3, TLR7, TLR8 and TLR9) receptors (Netea *et al*., 2008). Recognition of fungi by TLRs triggers the induction of numerous cytokines and chemokines through the interaction with the adaptor molecule Myd88 (myeloid differentiation primary response protein 88). Besides TLRs are not the central PRRs involved in antifungal immunity in humans, in immunocompromised hosts, polymorphisms in the TLR genes can result in a predisposition to fungal infections (Plato *et al*., 2015).

The CLRs family includes dectin-1*,* complement receptors, and macrophage mannose receptor. Less well-described include DC-specific ICAM3-grabbing non-integrin, dectin-2, DCL-1, Mincle, langerin and the mannose binding lectin (Denning *et al*., 2014). Undoubtedly, dectin-1 is the principal PRR, which recognizes β-glucans.

CLRs, in response to fungi, recognise both endogenous and exogenous ligands in the regulation of homeostasis and immunity. Dectin-1 induce cytokine and chemokine production including TNF, IL-2, IL-10, CXCL2 as well as IL-1β, IL-6 and IL-23 (Plato *et al*., 2015).

During infection, TLRs and CLRs are both required for antifungal responses, and these pathways interact to induce optimal immunity. When these immune defences fail

opportunistic fungal pathogens can establish potentially life-threatening infections (Plato *et al*., 2015).

Nevertheless, the fully integrated response to a specific pathogen depends on the mosaic of PRRs and receptor complexes that are engaged (Netea *et al*., 2008).

1.3.1.2 Fungal pathogen-associated molecular patterns (PAMPs)

Innate immune mechanisms are used by the host to respond to a range of pathogens in a rapid and conserved manner.

The fungal cell wall can be described as a dynamic, highly organized organelle that determines both the shape and viability of the fungus (Van de Veerdonk *et al.,* 2008). Components of fungal cell wall act as fungal PAMPs that are identified by PRRs. In the early time, proteins were considered the major drivers of the immune response, although polysaccharides and even lipids have emerged as important molecules in fungal immunology (Latgé, 2015). The three major cell wall components, found in all medically important fungi, are β-glucans, especially β-(1,3)-glucans, chitin; and mannans (chains of several hundred mannose molecules that are added to fungal proteins via N- or O-linkages) (Romani, 2011).

During the fungal infection, multiple host PRRs are likely to be stimulated by fungal PAMPs in different combinations depending on the fungal species, the host cell types, and even the same fungi can set differential expression of PAMPs (Romani, 2011).

However, fungi can mask or modify the cell wall components to prevent PRRs recognition. For example, besides β-1,3- glucans be highly immunostimulatory are often masked by less immunogenic structures in the outer cell wall (Plato *et al.*, 2015). Also, melanin pigments on the surface of *A. fumigatus* mask pamp-induced cytokine response (Latgé, 2010).

1.3.2 Macrophages immune response to fungal infections

Macrophages are a heterogeneous population that express the machinery for antigen presentation. However, their main contribution to antifungal defence is phagocytosis and killing of fungi. Although, fungi have various mechanisms or putative virulence factors to elude phagocytosis, escape destruction and survive inside macrophages. Moreover, the dimorphic fungi can multiply on macrophages and disseminate from the lungs to other organs (Romani, 2004).

The recognition of fungi by PRRs leads directly activation or to their internalization through the actin dependent process of phagocytosis (Eduard, 2009). Therefore, recognition and internalization of yeasts and conidia occurs mainly by coiling

phagocytosis, while entry of hyphae occurs by zipper-type phagocytosis. The coiling phagocytosis is a mechanism for the uptake of eukaryotic microorganisms by phagocytic cells, as macrophages, in which unilateral pseudopods wrap around microorganisms in multiple turns, giving rise to a largely self-apposed pseudopodal surfaces. Meanwhile, zipper-type occurs by sequential interactions between receptors and ligands on the surfaces of the pathogens and phagocytes, and then the pseudopods strictly follow the contour of the particle, embodying it (Romani, 2004).

The internalization of the fungal particle results in the formation of an intracellular vacuole called phagosome. The newly phagosome is innocuous, only then maturates after several sequential steps involving extensive vesicle fission and fusion events (mainly with components of the endosomal network), becoming phagolysosome. The phagolysosome is a compartment with potential antimicrobial activities, where the internalized fungi can be killed and digested (Brown, 2011).

Phagosomes, after internalization, undergo extensive remodelling and acquire microbicidal and lytic enzymes which leads to the progressive acidification of the phagosome lumen and the antimicrobial agents.

Thus, phagocytic cells employ oxidative and non-oxidative mechanisms working synergistically to kill extracellular and internalized fungi, which activation is greatly influenced by the state of cellular activation, controlled mainly, but not exclusively, through the actions of cytokines and other mediators of inflammation. Different phagocytes exploit distinct strategies to kill or restrict fungal growth, and these activities are also dependent on the fungal species involved (Brown, 2011).

One of this mechanism of anti-fungal defence is the production of reactive oxygen intermediates (ROI), mediated though a multi-component protein complex, the NADPH oxidase, which transfers electrons from NADPH to O_2 on the membrane of phagosome (Brown, 2011). The second major defence mechanism is inducible nitric oxide synthase (iNOS), expressed in the plasma membrane after activation of the macrophage (Pluddemann *et al*, 2011).

However, mammals have other mechanisms as the production of antifungal antimicrobial peptides (AMP). Lysozyme, a phagolysosome hydrolytic enzyme with activity against fungi, capable of killing or inhibit fungal growth through the enzymatic hydrolysis of *N*-glycosidic bonds present on fungal cell wall and/or by injury their membrane. Likewise, phagocyte cells can restrict nutrients availability, such as iron, removing it from the phagosome, through sequestration by lactoferrin, down regulation of transferring receptors and by transporter proteins (Brown, 2011).

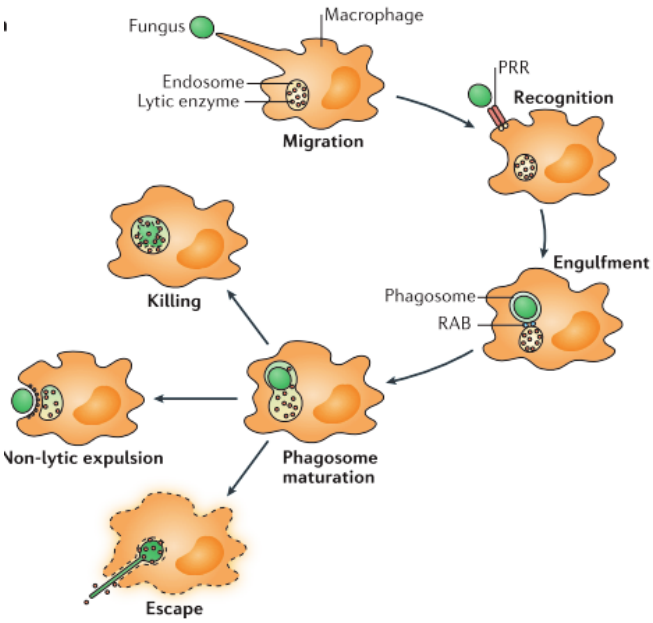

Figure 3: Macrophage-fungus interaction. The phagocytosis of the fungus into a phagosome compartment result in the killing of the pathogen or survival by various mechanisms, the non-lytic expulsion, or cause macrophage lysis by piercing the phagocyte membrane or through the induction of pyroptosis. (Adapted from Erwig & Gow, 2016)

Most pathogens are killed and degraded in mature phagolysosomes, but several fungal pathogens, including *H. capsulatum*, *C. neoformans*, *C. glabrata* and *C. albicans*, have mechanisms to survive, escape (Figure 3) or subvert the phagosome maturation process. Moreover, a substantial problem to immune system is the physical size of fungal cells, therefore, internalization of hyphal forming fungi causes low levels of phagocyte survival.

The mechanisms used by some fungi rely on hydrophobins, a thin coating of regulatory arranged RodAp hydrophobins (Latgé, 2010), and also melanin has been reported. Melanised cells are less susceptible to microbicidal peptides and to, ingestion by macrophages (Enjalbert *et al*., 2006); also, are less killed by alveolar macrophages, once melanins are charged polymers and phagocytosis is inversely correlated with cell charge (Langfelder *et al*., 2003).

In addition, it was shown a strong temporal association between intra-phagocytic hyphal growth and macrophage lysis. Hyphae are able to escape from phagocytes by growing and consequently lysing the infected cell. Pyroptosis (Figure 3) is one of several programmed cell death pathways that result in lytic cell death and was originally identified in macrophages infected with intra- cellular bacteria that were known to interfere with phagosome maturation, resulting in the release of cytokines signals to attract other immune cells to fight the infection.

1.4 Aims

Understanding how the fungal cell wall components are modulated and all their different actions on the host is an exciting challenge, setting the stage for new approaches to the treatment of fungal diseases.

This work has as the main goal of studying the immunomodulatory effect of the different components of the *A. infectoria* cell wall. Given the complexity of studying the interaction of filamentous fungi with cells of the host innate immune system it was also an important objective of this work to develop and characterise fungal cell wall nanoparticles in which the components were modulated and, this way, to design a novel model to study the interaction of macrophages with *A. infectoria* cell wall.

Chapter 2

Materials and Methods

2. Materials and Methods

2.1 Fungal Strains

The IMF006 *A. infectoria* strain used in this study was obtained from CBS-KNAW Fungal Biodiversity Centre, Utrecht, The Netherlands (reference CBS 137.9).

2.1.1. Fungal Culture media and Solutions

Fungal cultures were grown on potato dextrose agar (PDA; Difco) or yeast-malt extract (YME) medium with 4 % yeast extract, yeast extract (A1202-HA, Panreac-Cultimed) (w/v), 10 % malt extract (8266, BD) (w/v) and 10 % glucose (G8270, Sigma-Aldrich) (w/v). The growth media were prepared according to the manufacturer's instructions, sterilized by autoclaving (121 ºC, 1.2 atm for 20 min). Then, PDA were distributed into Petri dishes (Corning) while the liquid medium, YME, were distributed on sterile Erlenmeyer flacks' (Anjos *et al*., 2012).

2.1.1. Fungal Growth Conditions

A. Infectoria grew 2 weeks on PDA plates at 30ºC with an alternating 8 h light and 16 h dark (day-night) cycle under a blacklight lamp (F15W T8BLB; Grainger). Then the mycelium was submerged in liquid YME medium and scraped with an inoculation loop, and the homogenate used as inoculum. Liquid *A. infectoria* cultures were cultivated on YME at 30 ºC with constant orbital shaking at 120 rpm and by use of the day-night light cycle described above (Fernandes *et al*., 2016).

To inhibit the synthesis of melanin, it was used pyroquilon ((1,2,5,6-tetrahydropyrrolo [3,2,1,-ij]quinolin-4- one; Sigma®), a DHN-melanin synthesis inhibitor. Therefore, the liquid *A. infectoria* collected from PDA plates as described before were cultivate on YME with 50 µg/mL pyroquilon at 30 ºC with constant orbital shaking at 120 rpm and by use of day-night cycle described above (Fernandes *et al*., 2016). Likewise, to modulate the grow of fungus and change composition on the cell wall content in chitin and in glucans, *A. infectoria* were cultivated on liquid YME with 0,5 µg/mL nikkomycin (from *Streptomyces tendae*, N8028, Sigma®) or 1 µg/mL caspofungin (a gift from Merck & Co, Inc., Rahway, NJ, material transfer agreement no. 37006), respectively an inhibitor of chitin synthases and an inhibitor of and β-(1,3)-glucan synthase.

2.1.3. Quantification of chitin and β-(1,3)-glucan content on the cell wall of *A. infectoria* treated with nikkomycin

The chitin content on *A. infectoria* cell wall were quantified based on measurement of glucosamine (Merck ®) released by acid hydrolysis of purified cell walls. The quantification of the β-(1,3)-glucan were accomplished using the Aniline Blue Assay (diammonium salt, 415049, Sigma ®) with minor changes, as described previously (Fernandes *et al*., 2014).

2.1.3. *A. infectoria* harvest

The mycelial mats were harvested by filtration in a steel filter, then washed 4 times with distilled water, lyophilized, and froze at -20 ºC until the next step.

2.2. Preparation of nanoparticles of the cell wall of *A. infectoria*

2.2.1. *A. infectoria* cell wall isolation and nanoparticles preparation

The methodology used to obtain nanoparticles from fungal cell walls of *A. infectoria* (Cell Wall NanoParticles - CWNPs) was based on the described by François (2006). Firstly, *A. infectoria* mycelia were hydrated with few drops of distilled water and then ground in liquid nitrogen until a powder was obtained. The mycelia powder obtained were transfer to 2 mL eppendorf tubes with 10 mM Tris-HCl pH 8.0, 1 mM EDTA (TE), and centrifuged at 1,000 *xg* for 1 min. The supernatant was discarded, while the pellet was resuspended in TE plus a protease inhibitor cocktail (P8215, Sigma-Aldrich) and was transferred to 1.5 mL eppendorf tubes, each one containing 1 g of acid-washed beads (425-600 µm) (G8772, Sigma-Aldrich). Secondly, cell disruption using Magna Lyser® (Roche) were carried out, by applying four cycles of 4,800 rpm for 20 seconds (with 30 seconds' intervals on ice between cell disruption cycles). Thirdly, a centrifugation at 1,000 *xg* for 1 min was perform, and the supernatant collected. At the same time, 1 mL of TE plus protease inhibitor cocktail was added to the previously 1.5 mL eppendorfs (containing acid-washed beads and pellet), and a new round of cell disruption were accomplished. Then, a centrifugation at 1,000 *xg* for 1 min were performed, and the supernatant collected to the same falcon. Therefore, 1 mL of TE plus protease inhibitor cocktail was added to the Eppendorf tube, vortexed and centrifuged at 500 *xg* for 1 min. The obtained supernatant was collected and this wash step repeated six more times. Fourthly, the sum of supernatants obtained were centrifuged at 4,800 *xg* for 15 min, and the pellet resuspended in 1 mL TE. To finish, the resuspended pellet was centrifuge at 3,000 *xg* for 5 min, and the supernatant collected and dried overnight at 100 ºC on glass

test tubes. To finish, the CWNPs were resuspended on distilled water and conserved at -20 ºC.

2.2.2. Flow Cytometry of CWNPs

Flow cytometry analysis were performed on Partec CyFlow® space instrument, at the CNC Flow Cytometry Core Facility. This analysis allowed the assessment of population dispersion, trough the relation between the forward-scattered light (FSC), which is proportional to the area and size of the particles, and the side-scattered light (SSC), which is proportional to internal complexity. The analysis of sample CWNPs concentration using the method of True Volumetric Absolute Counting is based on the precise measurement of a fixed volume by means of two platinum electrodes. Flow cytometry uses the measurements of the light scattering, which occurs when a particle deflects incident laser light; the extent depends on the physical properties of a particle, namely, its size and internal complexity.

To execute this analysis, the CWNPs were centrifuged 4,800 *xg* for 15 min and the pellet resuspended on RPMI (R4130 SIGMA® RPMI-1640 Medium), and sonicated. Then, labelled with 0,5 µg/mL Flurorescein (FITC) (Alexa Fluor® 488 dye, ThermoFisher Scientific®) with 2 h incubation, and before taking the samples to the cytometer they were sonicated again. The software used on the analysis is FloMax® 2.62.

2.2.3. Zeta potential of CWNPs

One of the aspects to consider is the zeta potential. Zeta potential analysis is a technique for determining the surface charge of nanoparticles in solution (colloids) and it is closely related to suspensions stability and particle surface morphology. CWNPs have a surface charge that attracts a thin layer of ions of opposite charge to the nanoparticle surface. Furthermore, nanoparticles with zeta potential values above +25 mV or less than -25 mV typically have high degrees of stability. Dispersions with a low zeta potential value will eventually aggregate due to Van Der Waals inter-particle attractions.

Zeta potential measurement were carried out to characterize the isolated cell wall from *A. infectoria* mycelia using Beckman Coulter® DelsaTM Nano C Particle Analyser and the particles' size, which allow us the analysis not only the zeta potential but also the size.

To calibrate the equipment, it was used a standard control (Otsuka Electronics, Osaka, Japan), while the CWNPs was centrifuged by 4,800 *xg* for 15 min and the pellet resuspended by adding RPMI (Sigma R4130) and processed by ultrasound. Zeta

potential measurement of the CWNPs were achieved (Beckman Coulter® DelsaTM Nano C version 2.31/2.03 Software).

2.2.4. Transmission electron microscopy (TEM) to analyse the CWNPs

TEM is a versatile and powerful technology tool for imaging and diffraction of micrometer and sub-micrometer structures. In this work, this technology was used to study the structure of the CWNPs of *A. infectoria*, from the different growth conditions.

The suspensions of CWNPS were centrifuged at 3000 rpm for 3 min to form a pellet. The pellet CWNPs were fixed with 2.5 % glutaraldehyde in 0.1 M sodium cacodylate buffer (pH 7.2) for 2 h. Following rinsing in the same buffer, post-fixation was performed using 1 % osmium tetroxide for 1 h. After rinsing in distilled water, CWNPs were dehydrated in a graded ethanol series (30–100 %), impregnated and embedded in Epoxy resin (Fluka Analytical). Ultrathin sections (~70 nm) were mounted on copper grids and stained with lead citrate 0.2 %, for 7 min. Observations were carried out on a FEI-Tecnai G2 Spirit Bio Twin at 100 kV.

2.3 Macrophages-NPs interaction assays

2.3.1 Macrophages Cell Line

The macrophage cell line used in this research was the RAW 264.7 mouse macrophage cell line from the European Collection of Cell Cultures (ECACC catalog number 91062702; Salisbury, UK).

2.3.2. Cell culture

The macrophage cell line grew in Dulbecco's modified Eagle's medium (DMEM; Sigma-Aldrich) supplemented with 10% inactivated Fetal Bovine Serum (FBS; Life Technologies), 10 mM Hepes, 12 mM sodium bicarbonate and 11mg/mL sodium pyruvate (S8636, Sigma-Aldrich).

The cell culture was maintained in 75 cm^2 flasks (Corning) using 25 mL of medium and in a humidified atmosphere with 5 % CO_2 at 37 ºC. On routine maintenance in culture, cells were seeded at a confluence of estimated 10 % and grown to a confluence of approximately 70 %. All the experiments here described were performed with cells between passages 10 and 16.

Phosphate Buffered Saline solution (PBS buffer: 10 mM Na_2PO_4; 1.8 mM KH_2PO_4; 137 mM NaCl; 2.7 mM KCl at pH 7.4) was used to wash the macrophage cells.

RPMI (R4130 SIGMA® RPMI-1640 Medium) supplemented with 10 % inactivated FBS, 23.8 mM sodium bicarbonate and 50 mM glucose were used as medium for interaction assays described below.

2.3.3 Interaction of *A. infectoria* CWNPs with macrophages

The interaction assays were performed using the CWNPs (prepared as described on section 2.2.1.) and macrophages (grew as described on section 2.3.2.). The macrophages were plated on multiwells (Corning) for 30 min, 1h30 min, 3 h and 6 h at 37 ºC in a 5 % CO_2 atmosphere. The macrophages were placed on 24-mm, with 12 mm cover-slips, with a cell density of 1,25 x 10^5 cells/mL in RPMI. The expected macrophage density at the day of infection was to be approximately of 2.5 x 10^5 cells/mL.

Prior to interaction, the CWNPs were sonicated to ensure that the particles were not aggregated while interacting with the macrophages. Then, the CWNPs were centrifuged at 4,800 *xg* for 15 min and the pellet resuspended on RPMI. The macrophages were washed twice with 37 ºC-pre-heated PBS and the culture medium renewed. The CWNPs were added to RAW 264.7 cell culture in a ratio of 1:1 (one nanoparticle to one macrophage).

2.3.4. Transmission Electron Microscopy (TEM) assay

TEM was used to study the interaction between macrophages and the cell wall nanoparticles cell wall of *A. infectoria* grown under control conditions (ctCWNPs) at the ultrastructure level. The interaction between the macrophages and the ctCWNPs (prepared as described on section 2.2.1.) and macrophages (grew as described on section 2.3.2.) proceeded as described in section 2.3.3. Although, the macrophages were added to 96-well plate with a cell density of 1.25 x 10^5 cells/mL in RPMI. The expected macrophages density at the day of infection would be approximately of 2.5 x 105 cells/mL.

After 3 h, the culture medium was removed from the wells and washed with PBS. The macrophages were fixed with 2.5 % glutaraldehyde in 0.1 M sodium cacodylate buffer (pH 7.2) for 2 h. Post fixation was performed using 1 % osmium tetroxide for 1 h. Then, the cells were removed by scratching from the support using pipette tip. Further, they were rinsed in buffer, buffer and distilled water and a final rinsing step in distilled water, 1 % aqueous uranyl acetate was added to the cells, for 1h in the dark, for contrast enhancement. After rinsing in distilled water, samples were dehydrated in a graded ethanol series (30–100 %), impregnated and embedded in Epoxy resin (Fluka Analytical). Ultrathin sections (~70 nm) were mounted on copper grids and stained with

lead citrate 0.2 %, for 7 min. Observations were carried out on a FEI-Tecnai G2 Spirit Bio Twin at 100 kV.

2.3.5. Fluorescence microscopy assay

Fluorescence microscopy was used to study macrophage morphology after the interaction with the *A. infectoria* cell walls nanoparticles grown with pyroquilon (pyrCWNPs) or under control conditions (ctCWNPs). For that, the macrophages cytoplasmic membrane was probed with WGA (Wheat Germ Agglutinin) Alexa Fluor® 350 conjugate and the deoxyribonucleic acid with DAPI (4',6-Diamidino-2-Phenylindole, Dihydrochloride) (Eugene®, Oregon USA; D1306).

The CWNPs were prepared as described in section 2.2.1 and macrophage cells were grown as described in section 2.3.2, respectively. And, CWNPs were added to RAW 264.7 cell cultures as described in section 2.2.3..

After 30 min, 1 h 30 min, 3 h and 6 h the 24-well plates were put on ice, while the cover-slips were washed twice with cold PBS and then fixed with 4 % paraformaldehyde (S233998, Sigma-Aldrich) in PBS for 15 min at room temperature. The fixed cells were again washed twice with cold PBS, followed by a 10 min incubation in the dark with 0,01 mg/mL WGA in PBS (W7024, Invitrogen®).

Finally, the cells were incubated with DAPI 0.02 % for 10 min at room temperature.

Afterwards, the cells were washed three times with PBS and the cover-slips were mounted on glass slides, using a fluorescent mounting medium, termed DAKO (DakoCytomation Fluorescent Mounting Medium) (S3023, Luso Patex Medical).

The cell imaging was performed on a Carl Zeiss LSM 710 Confocal Microscope Confocal Microscope, using a 63x Plan-ApoChromat (NA 1.4) oil objective. Image analysis was achieved using the Fiji software.

2.3.6. Viability test

Trypan Blue is one of the most commonly used dye to assess cell viability by a dye exclusion assay, based on the principle that an intact cell, with an intact cytoplasmic membrane, does not allows the entrance of certain dyes.

Briefly, the CWNPs of *A. infectoria* were prepared as described in section 2.2.1. and macrophages were grown as described in section 2.3.2. The interaction assay was performed as described on section 2.2.3., although, macrophages were added to 96-well multiwell with a cell density of 1.25×10^5 cells/mL in RPMI. The expected macrophages density at the day of infection would be approximately of 2.5×10^5 cells/mL.

The viability test was performed after the collection of the macrophages by scratching and staining the cells with 4 % Trypan Blue (T8154, Sigma®) diluted in PBS (Freshney, 1994).

2.3.7. Fluorescence Microscopy assay for chitin of the CWNPs and macrophages acidic organelles

With the purpose of describing the morphology changes on macrophages during the interaction with the different nanoparticles and to determine how the interaction happen, a fluorescence microscopy approach was used.

For that, the CWNPs of *A. infectoria* were prepared as described in section 2.2.1 and macrophage cells were grown as described in section 2.3.2, respectively. CWNPs were added to RAW 264.7 cell cultures as described in section 2.2.3..

Before the interaction, the CWNPs were labelled with 0,1 % CalcoFluor White (CFW) (Flurescent Brightener 28, Sigma®) during 30 min of incubation on dark. While, to label the macrophages it was used LysoTracker Red® (Red DND-99, Invitrogen. Molecular Probes®) during 1 h 30 min incubation at 37 ºC.

After 30 min, 1 h 30 min, 3 h and 6 h the 24-well plates were put on ice, the cover-slips on the wells were washed twice with PBS and then fixed with 4 % paraformaldehyde (S233998, Sigma-Aldrich) in PBS for 15 min at room temperature. The fixed cells were again washed twice with cold PBS.

Then, the cover-slips were mounted on glass slides, using a fluorescent mounting medium, termed DAKO (S3023, Luso Patex Medical).

The cell imaging was performed on a Carl Zeiss LSM 710 Confocal Microscope, using a 63x Plan-ApoChromat (NA 1.4) oil objective. Lastly, the analysis was achieved using Fiji software, with Plugging Cell Counter and 3D Viewer.

2.3.8. Relative quantification of TNF-alpha gene (Tumor necrosis factor alpha gene) expression in macrophages

Once activated macrophages change the expression of several genes coding for signalling factors, such as TNF-α, coded by the gene TNF-alpha. The TNF-alpha mRNA was quantified as a measure of the activation of macrophages during the interaction with CWNPs of *A. infectoria* growth with different cell wall components inhibitors (caspofungin, nikkomycin and pyroquilon) or from the growth under control conditions. CWNPs of *A. infectoria,* prepared as described in previous sections, were added to RAW 264.7 cell cultures as described in section 2.2.3.. In these experiments, the macrophages were added to the 6-well plates with at a cell density of 5 x 10^5 cells/mL in RPMI. The

expected macrophages density at the day of infection would be approximately of 1 x 10^6 cells/mL.

After 1 h and 3 h, macrophages were scraped and transferred to falcon tubes, after centrifugation at 10 000 *xg* for 5 min, the pellet were resuspended in PBS and centrifuged again and the pellet resuspended with PBS.

RNA extraction was performed with the NucleoSpin® RNA Kit protocol (Macherey-Nagel, 740955) according to the manufacturer's instructions. Concentrations of RNA were determined by the A260/280 value of the sample on NanoDrop 2000 (Thermo Fisher Scientific™).

Then, were performed the reverse transcription of total RNA to processed it into cDNA using a Transcriptor First Strand cDNA synthesis Kit (04896866001, Roche®), according to the kit instructions. The reverse transcription reaction was performed in a GeneAmp PCR System 2400 (PerkinElmerTM), with the followed programme: 25 ºC for 10 min, 50 ºC for 60 min; 85 ºC for 5 min, and lastly, completion at 4 ºC.

To quantify the relative gene expression of TNF-α we proceeded to real-time quantitative RT-PCR, using the SsoFast™Eva Green®Supermix (BioRad Laboratories, Inc) in the LightCycler® II thermocycler (Roche®) according to the manufacturer's instructions. Primers for TNF-apha and for GAPDH (Table 1) were used in a concentration of 0.5 µM. The process of quantitative Real Time PCR was accomplished using the LightCycler® II instrument (Roche, Portugal, Software LightCycler 2.0), with specific thermal programme steps (Table 2).

The analyse of the gene amplification for quantification of relative expression was proceed based on the ration of Ct values with the normalization against GAPDH, using the $2^{-\Delta\Delta Ct}$ method (Livak & Schmittgen, 2008). The Ct concerns the first cycle amplification, which corresponds to the cDNA fragment that was detected above the baseline.

Table 3 Oligonucleotides sequences used in quantitative Real Time PCR

Gene	Primer	5' → 3' sequence	Reference	Amplicon size (bp)
TNF-α	**Forward**	5-CATGATCCGCGACGTGGAACTG-3'	Gosh *et* al., 2010	195
	Reverse	5'-AGAGGGAGGCCATTTGGGAACT-3'		
GAPDH	**Forward**	5'-GTCTTCACCACCATGGAGA-3'	Chehadeh *et al*., 2001	260
	Reverse	5'-CCAAAGTTGTCATGGATGACC-3'		

Table 4 Quantitative Real Time PCR parameters for amplification

Gene	Step		Temperature (ºC)	Duration
TNF-α	Enzyme Activation		95	30 sec
	40 cycles	Denaturation	95	5 sec
		Annealing	60	5 sec
		Extension	72	20 sec
	Cooling		4	∞
GAPDH	Enzyme activation		95	30 sec
	40 cycles	Denaturation	95	5 sec
		Annealing	55	5 sec
		Extension	72	20 sec
	Cooling		4	∞

2.4. Statistical Analysis

Data were analysed by Student's two tailed test (unpaired teste), in order to compare two groups, using Prism (version 6) software (GraphPad Software, Inc., La Jolla, CA). Data are presented as the means ± standard errors of the means (SEMs) or standard deviations (SDs), and differences were considered significant at P values of <0.05. At least three samples were used for three independent experiments.

Chapter 3

Results

3. Results

3.1. Nanoparticles characterization

3.2.1. Differential Fungal Growth

In order to modulate the cell wall of *A. infectoria* components content, the fungus was grown with different compounds as describe in Chapter 2 (Materials and Methods).

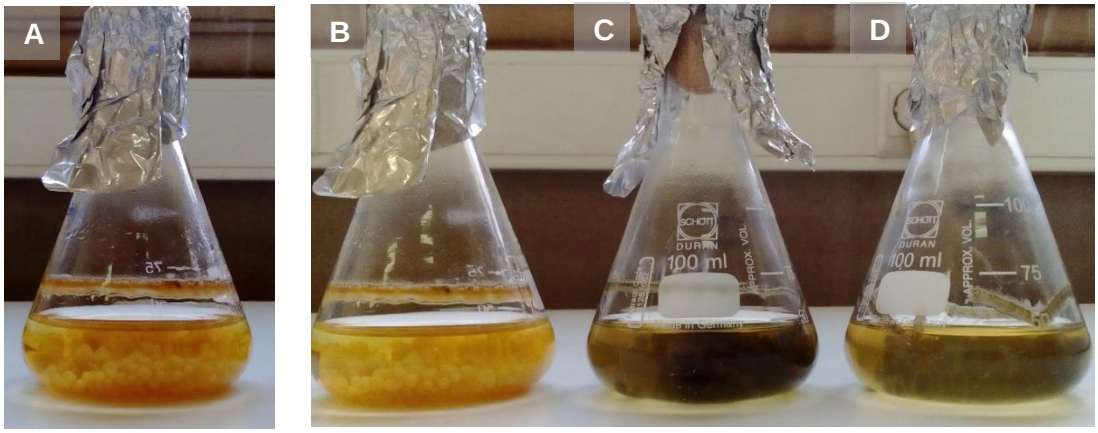

Figure 4: Growth of *A. infectoria* mycelia with different compounds. *A. infectoria* cultured on YME liquid media at 30 ºC under constant orbital shaking at 120 rpm 3 days with alternating 8-h light and 16-h dark periods under a blacklight lamp for 3 days. *A. infectoria* was cultivated in YME /A); in YME with 50 µg/mL pyroquilon (B); in YME with 0,5 µg/mL nikkomycin (C); in YME with 1 µg/mL caspofungin (D).

Macroscopically it could be observed differences in the colour and morphology of the mycelia (Figure 4), depending on the fungal growth condition. The *A. infectoria* grown with 50 µg/mL pyroquilon presents a lighter colour but with a morphology similar to the control mycelia. When grown with 0.5 µg/mL nikkomycin, the mycelia present a darker colour (almost black), with no differences on the fungal morphology. On the other hand, the growth in the presence of 1 µg/mL caspofungin lead to a different, darker colour than the control, but lighter than that observed with the nikkomycin grown *A. infectoria*.

3.1.2. Chitin and β-(1,3)-glucan content on *A. infectoria* cell wall grown with nikkomycin

To determine the changes caused by nikkomycin in *A. infectoria* cell wall components content, were measured the variations of the cell wall components, glucan and chitin (by quantifying the glucosamine content, the end hydrolytic product of chitin), when the fungus is grown with 0.5 µg/mL or with 1 µg/mL of nikkomycin.

The results showed that when compared with the control growth conditions, the percentage of glucan decreases with both concentrations of the nikkomycin (Figure 5).

Otherwise, when *A. infectoria* was grown with 0.5 µg/mL or 1 µg/mL nikkomycin, the cell wall content in glucosamine, a measure of the chitin cell wall content, increased when compared with the control fungal cultures, in the absence of nikkomycin, a chitin synthase inhibitor

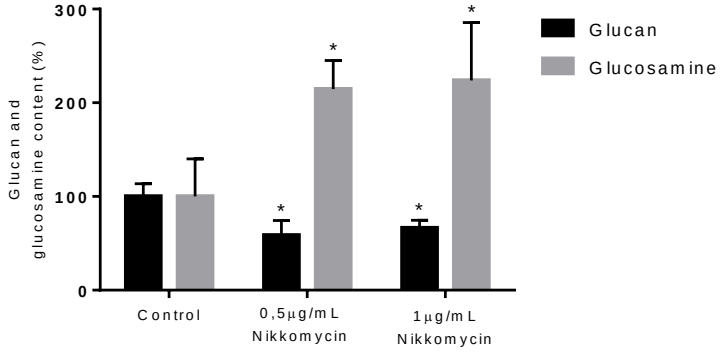

Figure 5: Modulation of cell wall components by nikkomycin. *A. infectoria* cultured on YME at 30 ºC under constant orbital shaking at 120 rpm 3 days with alternating 8-h light and 16-h dark periods under a blacklight lamp for 3 days. YME without (control) or with 0,5 µg/mL or 1 µg/mL nikkomycin. The chitin and glucan content is normalized to the fungal biomass and expressed as a percentage of chitin or glucan content of the control. Results are the mean ± the standard error of the mean of triplicates of three independent experiments (Student's t test). *, P<0,05; **, P<0.03; ***, P<0.01.

3.1.3. Flow Cytometry characterization of nanoparticles prepared from the fungal cell wall of A. *infectoria* - CWNPs

In order to characterize the nanoparticles of cell wall of *A. infectoria* grown under control conditions (ctCWNPs) and of *A. infectoria* grown with pyroquilon (pyrCWNPs), caspofungin (caspCWNPs) and nikkomycin (nkCWNPs), we used a flow cytometry technique. The flow cytometry allows analysis of multiple physics characteristics of single particles, include the particle's relative size, relative granularity or internal complexity, and relative fluorescence intensity. Forward-scatter light (FSC) is proportional to surface area or size, while side-scattered light (SSC) is proportional to particle granularity or internal complexity. The correlation of the measurements of FSC and SSC allows the differentiation of particles types and heterogenous populations. This way, it was possible to understand if the CWNPs were different according to the differential growth with the analyse of size versus complexity of each population (Figure 6). The true volumetric absolute counting allowed the analysis of a fixed volume defined by the distance between two platinum electrodes. The CWNPs were detected due to their label with FITC, this way, with the channel FL1 (Figure 6) and with the count of events, the peak gave as the quantification of CWNPs concentration.

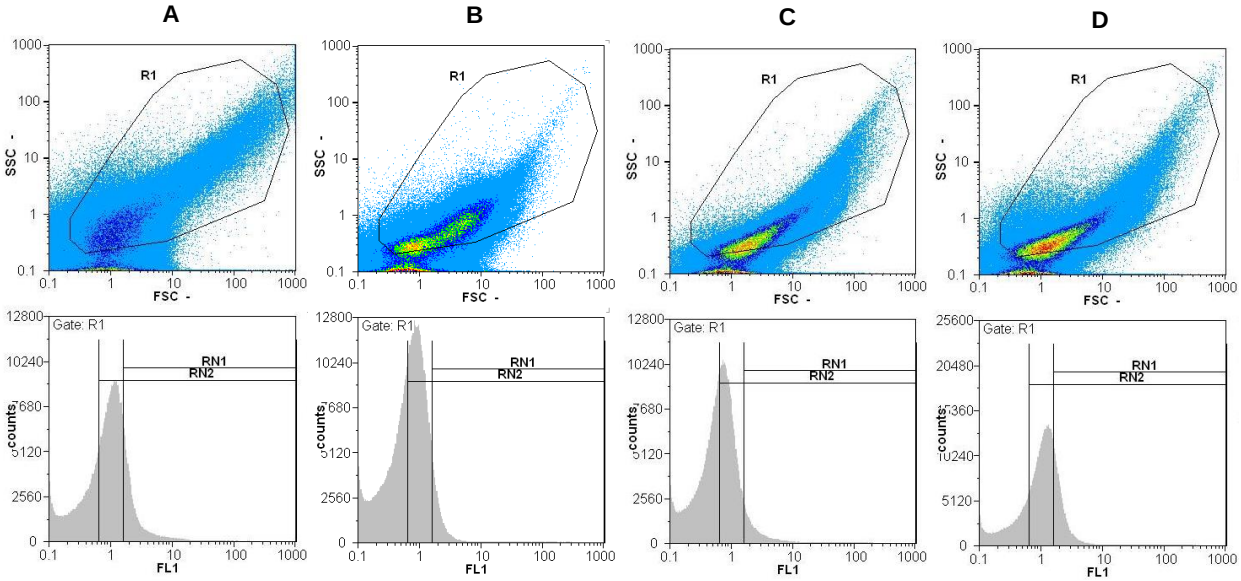

Figure 6: Flow cytometry signatures of the CWNPs. Analyzed on Partec Cyflow® of the CWNPs *A. infectoria*. The ctCWNPs (A), pyrCWNPs (B), casCWNPs (C) and nkCWNPs (D). The CWNPs were label with FITC (channel FL1). Events showed by forward-scattering light (FSC) and side-scattering light (SSC) were gated according to CWNPs discounting RPMI medium signal (R1). Under is the detection of FITC label in the CWNPs, which peak was used for concentration measurements through Volumetric Absolute Counting method.

The treatments along the growth of *A. infectoria* caused differences on the CWNPs constitution, acquiring different characteristics, observed by the different disposition of the CWNPs' population of each condition in study (Figure 6). Comparing the pyrCWNPs (B) with the ctCWNPs (A), it was found find that most of the nanoparticles are less internal complex and are generally small. The same happens with the caspCWNPs(C) and nkCWNPs (D).

3.1.4. Zeta potential and size of the CWNPs

The characterization of the CWNPs included the measurement of several physical properties using a Beckman Coulter® DelsaTM Nano C Particle Analyser (Table 1).

The data regarding the CWNPs' size was gathered trough dynamic light scattering (DLS), which the metric "particle diameter" is the most commonly descriptor of particle size. However, particles in dispersion may adhere to one another and form aggregates and increase the mean size. The caspCWNPs were the ones presenting smaller size values (138.5 ± 102.3 nm), unlike the ctCWNPs that had the highest diameter values (365.2 ± 72.5 nm). The polydispersity index (PDI) is also an information gathered by DLS. The PDI values are presented between 0 and 1, in which 0.1 represents a monodispersity; values higher than 0.1 indicate polydispersity; values between 0.1 and 0.25 indicates a narrow size particle distribution. The CWNPs of fungi exposed to the

compounds while growing had different PDI values when compared with the fungi grown in control conditions.

Table 3 Nanoparticles' size distribution and zeta potential analysed using the Beckman Coulter® DelsaTM Nano C Particle Analyser instrument

Growth conditions	Diameter (nm)	Polydispersity Index (PDI)	Zeta Potential (mV)	Mobility (cm^2/Vs)	E. field (V/cm)
Control	365.2 ± 72.5	0.177 ± 0.029	-10.91 ± 0.92	$-2.28 \times 10^{-5} \pm 0.73 \times 10^{-5}$	-14.29 ± 0.01
Pyroquilon	196.4 ± 12.3	0.316 ± 0.030	-7.85 ± 0.44 #	$-6.11 \times 10^{-5} \pm 0.34 \times 10^{-5}$ #	-14.35 ± 0.01
***C*aspofungin**	138.5 ± 102.3	0.231 ± 0.071	-7.17 ± 0.60 #	$-5.58 \times 10^{-5} \pm 0.47 \times 10^{-5}$ #	-14.44 ± 0.00
Nikkomycin	217.0 ± 60.8	0.246 ± 0.111	-3.65 ± 2.00 #	$-2.84 \times 10^{-5} \pm 1.56 \times 10^{-5}$ #	-14.38 ± 0.00

Analysis of the ctCWNPs (control), pyrCWNPs (pyroquilon), caspCWNPs (caspofungin) and nkCWNPs (nikkomycin). Average of triplicates ± SD of the mean; (Student's t test) #, P<0.007, relating growth conditions with control growth condition

Another parameter studied was the electric field, which is the electric field applied across the electrolyte, which attract the charged particles towards the electrode of opposite charge. The mobility, one of the physical properties studied, is the velocity of the particle in a unit electric field, and is measured when the particle moves towards the electrode; depends on particle size, the properties of the electrode solution in wish it is suspended, and the charge inside.

The zeta potential is a value related to suspensions stability and particle surface morphology. The layer surrounding the particle exists as two parts: an inner region (Stern layer) where the ions are strongly bound and an outer (diffuse) region where they are less associated. In the diffuse region, there is a boundary within the ions form a stable entity, when the particle moves, ions on the boundary moves. The potential at this boundary is the zeta potential. Suspension with large negative or positive (-25 or 25 mV), the particles tend to repel each other, while when zeta potential has low values there won't be any force to prevent the particles to come together.

The results obtained show that the CWNPs had similar electric field regardless of the growing conditions. However, the mobility values are a significantly different, resulting in different values of zeta potential of the pyrCWNPs, caspCWNPs or nkCWNPs. Anyhow, the zeta potential values for the different CWNPs are low (Table 1) (between -25 and 25 mV), being instable suspensions.

3.1.5. Analysis of the CWNPs morphology by TEM

To visually evaluate the impact of pyrCWNPs, caspCWNPs and nkCWNPs and ctCWNPs to complement the characterization of the nanoparticles, TEM was used to observe the ultrastructure of the CWNPs. As seen in Figure 7 TEM analysis indicates that CWNPs obtained are spherical particles and did not showed clear differences between the distinct CWNPs. It is worth mention that all the CWNPs, except for those nkCWNPs (D), are aggregated.

Using these same TEM images, a random diameter measurement was done (Table 4). The diameters values of the caspCWNPs, are significantly smaller than the ctCWNPs.

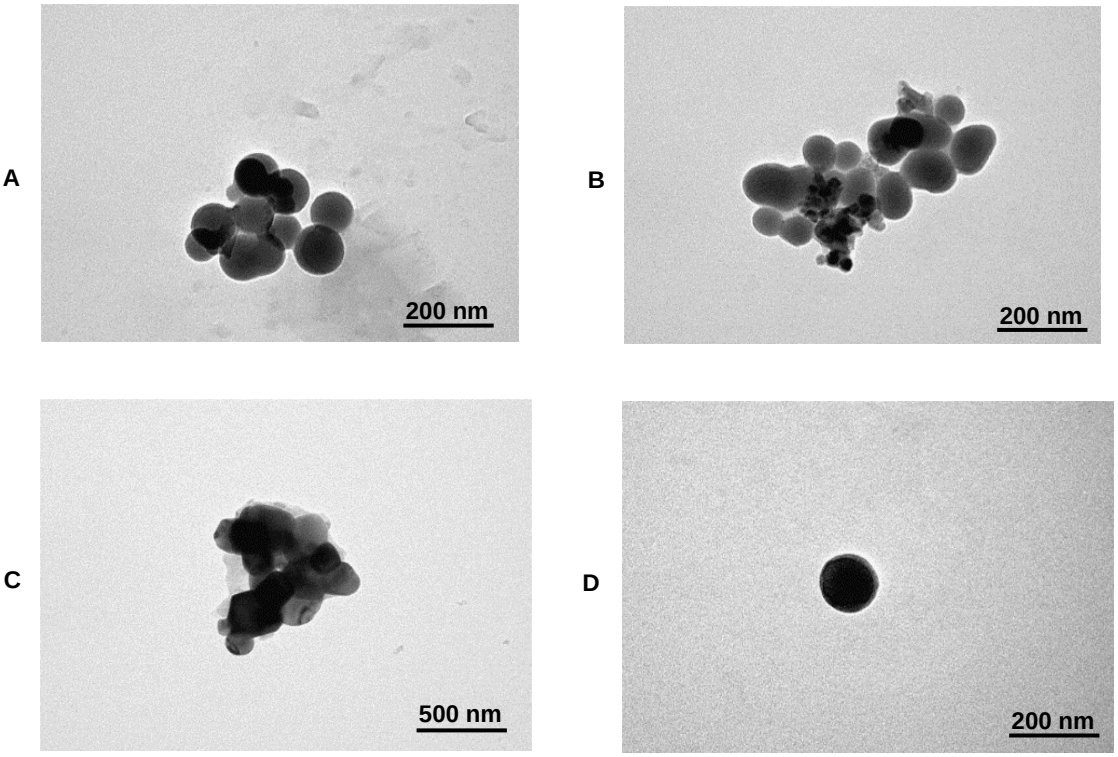

Figure 7: TEM images of CWNPs of *A. infectoria*. ctCWNPs (A), pyrCWNPs (B), caspCWNPs (C) nkCWNPs (D). Bars, 500 nm (C) and 200 nm (A, B and C). The images were obtained with FEI-Tecnai G2 Spirit Bio Twin transmission electron microscope at 100 kV.

Table 4 Nanoparticles diameter (nm) measured with FEI-Tecnai G2 Spirit Bio Twin transmission electron microscope at 100 kV

Growth conditions	Diameter (nm) * Means ± SD
Control	207.43 ± 130.95
Pyroquilon	78.65 ± 33.20 #
Caspofungin	70.19 ± 47.57 #
Nikkomycin	106.11

Analysis of the TEM images of ctCWNPs (control), pyrCWNPs (pyroquilon), caspCWNPs (caspofungin) and nkCWNPs (nikkomycin). Average ± SD of the mean; (Student's t test) #, P<0.05, relating CWNPs from fungi growth conditions with control growth condition

3.2. Interaction assays

3.2.1. TEM study on the interaction of ctCWNPs with macrophages

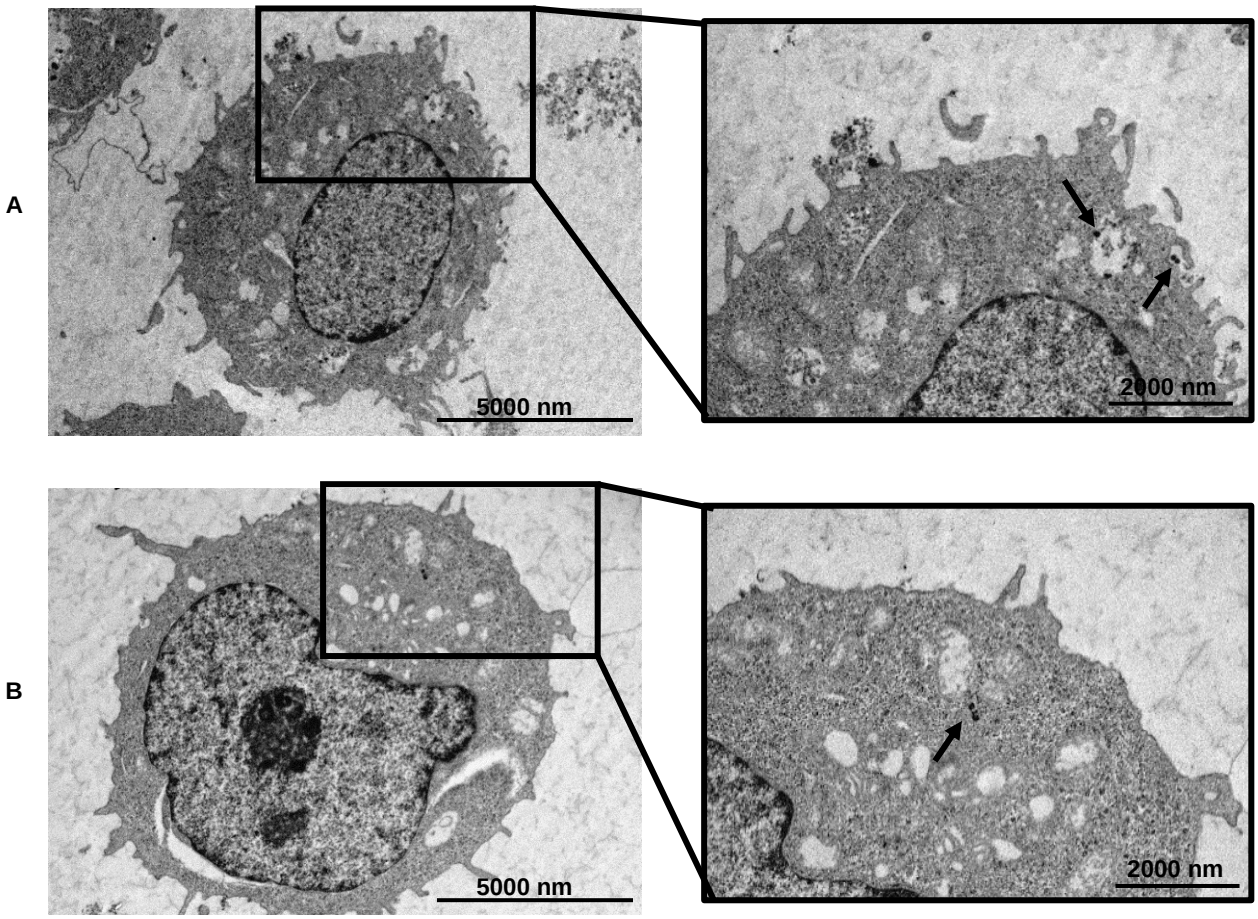

Figure 8: TEM observations of macrophages RAW 264.7 during the interaction with ctCWNPs during 3 h. Black arrows indicate the CWNPs localization. The images indicate that CWNPs are taken by the macrophages by endocytosis and can stay inside the macrophage in an internal compartment. But, the CWNPs can also be free in the macrophage cytoplasm (B). Scale bar indicates 5000 nm for the cell on the left panels and 2000 nm for the crops on the right panels. Several size measurements of the ctCWNPs were also made. The images were obtained with FEI-Tecnai G2 Spirit Bio Twin transmission electron microscope at 100 kV.

One important issue to be studied in this work was how the macrophages internalize the CWNPs. Obtaining TEM images of the macrophage during the interaction with the ctCWNPs, enable the characterization the model of interaction between macrophages and the CWNPs.

Using TEM, it was understood that the CWNPs are more electrodense than the biomaterials in the macrophage (Figure 8). In Figure 8A it is possible to observe that the macrophage exhibits pseudopods extensions to hold and internalize CWNPs (represented with the black arrows); in this same Figure 8A it is visible an intracellular compartment, delimited by a membrane, probably and endosome or a phagosome containing CWNPs. Otherwise, in Figure 8B nanoparticles are found in the macrophage's cytoplasm.

RAW 264.7 mouse macrophages show the typical morphology. Random measures (number of measures) of the CWNPs with FEI-Tecnai G2 Spirit Bio Twin transmission electron microscope at 100 kV, shows that CWNPs have a diameter of 213.15 ± 138.79 nm (mean ± SD).

3.2.2. Fluorescent microscopy assay for Sialic Acid and Deoxyribonucleic acid

To better understand the effect of pyroquilon, an inhibitor of DHN-melanin synthesis, in the response of macrophages to the CWNPs of *A. infectoria* namely an impact on macrophages' morphology, it was used WGA that probes for N-acetyl-D-glucosamine and sialic acid of the host cytoplasmic membrane, and DAPI that binds deoxyribonucleic acid, and is widely used to probe for cell nuclei (Figure 9). In this assay, the CWNPs were not marked, only the macrophages, with the fluorescence mostly present next to the cytoplasmic membrane.

Macrophages kept under control conditions (Figure 9), not exposed to fungal CWNPs, show a typical morphology, roundish. The same was observed during interaction with ctCWNPs, i.e. with no inhibitors of the cell wall components. However, when the macrophages were exposed to pyrCWNPs, a different result can be observed. The macrophages become enlarged and stretched. The nuclei labelling with DAPI did not show any noticeable difference in the three conditions studied.

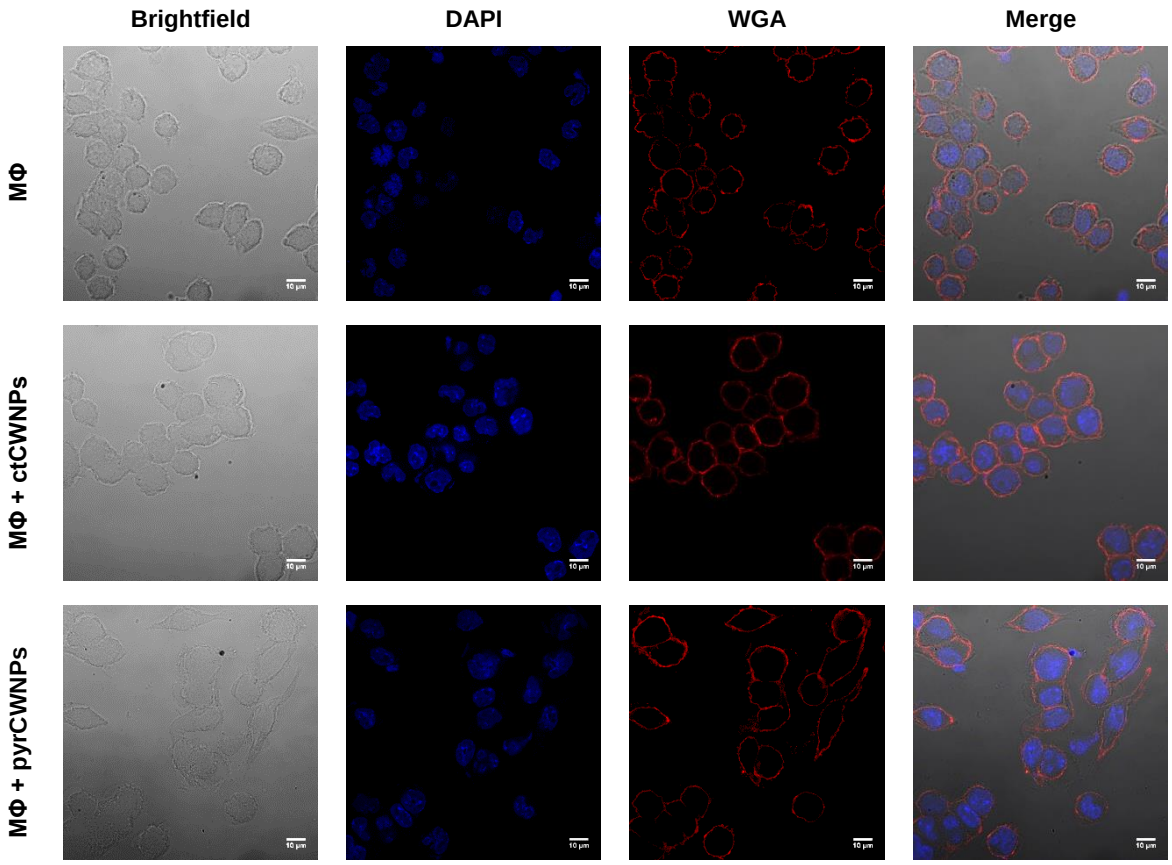

Figure 9: Macrophages morphology upon exposure to *A. infectoria* CWNPs. Macrophages that interacted with CWNPs of *A. infectoria* grown with 50 µg/mL pyroquilon (pyrCWNPs) or without (ctCWNPs) were labelled with WGA Alexa Fluor® 350 conjugated (W7024, Invitrogen®) and DAPI (Eugene®, Oregon USA; D1306). Scale bar indicates 10 µm. Cell imaging was performed on a Carl Zeiss LSM 710 Confocal Microscope, using a 63x PlanApoChromat (NA 1.4) oil objective.

3.2.4. Macrophages viability upon exposure to CWNPs

One of the main objectives of this work was to understand if different CWNPs which it was modulated the components had different immunomodulatory effect on macrophages. Besides the morphological changes already described, the work proceeded with the quantification of macrophages viability as a result of the relative activation by the different CWNPs prepared in this work. Therefore, macrophages response viability quantification was done using the Trypan blue assay, which identify the viable host cells with intact membranes since these are not able to take up the trypan blue dye.

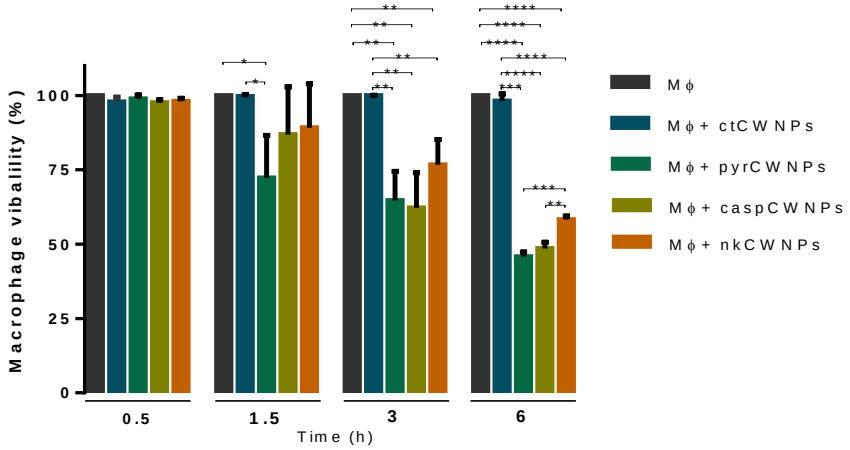

Figure 10: Macrophage viability during interaction with CWNPs. The percentage of viable macrophages were quantified using the Trypan Blue staining teste. Macrophages were exposed during 0.5, 1.5, 3 and 6 h to CWNPs of *A. infectori (*MΦ+ctCWNPs*) a* and *A. infectoria* grown with 50 µg/mL pyroquilon (MΦ+pyrCWNPs), with 1 µg/mL caspofungin (MΦ+caspCWNPs) or with 0,5 µg/mL nikkomycin (MΦ+nkCWNPs), with ratio 1:1. Results are the mean ± the standard error of the mean of triplicates of three independent experiments (Student's t test). *, P<0,04; **, P<0.03; ***, P<0.001; ****, P<0.0001.

In the beginning of the interaction of macrophages with the fungal CWNPs (30 min), the macrophages viability was similar in all conditions (Figure 10). However, higher periods of exposure lead to a different pattern of phagocytic cells dead, when these cells were in contact with fungal CWNPs prepared from *A. infectoria* grown in the presence of inhibitors of the cell wall components.

The inhibition of DHN-melanin by growing the fungus with pyroquilon was the only condition that at the 1.5 h-period of exposure, resulted in a decrease of the macrophages viability in 10 %. After 3 h-period of exposing the macrophages to different CWNPs a decreased viability was observed for all the conditions (except ctCWNPs).

At 6 h interaction, the CWNPs prepared from fungi grown either inhibitors caused a decrease around 20 % of the macrophages viability when compared with 3 h interaction (Figure 10). Unexpectedly, the ctCWNPs, during the 6 h interaction, did not change the viability of the macrophages population (Figure 10).

3.2.5. Internalization of CWNPs of *A. infectoria* and acidic organelles

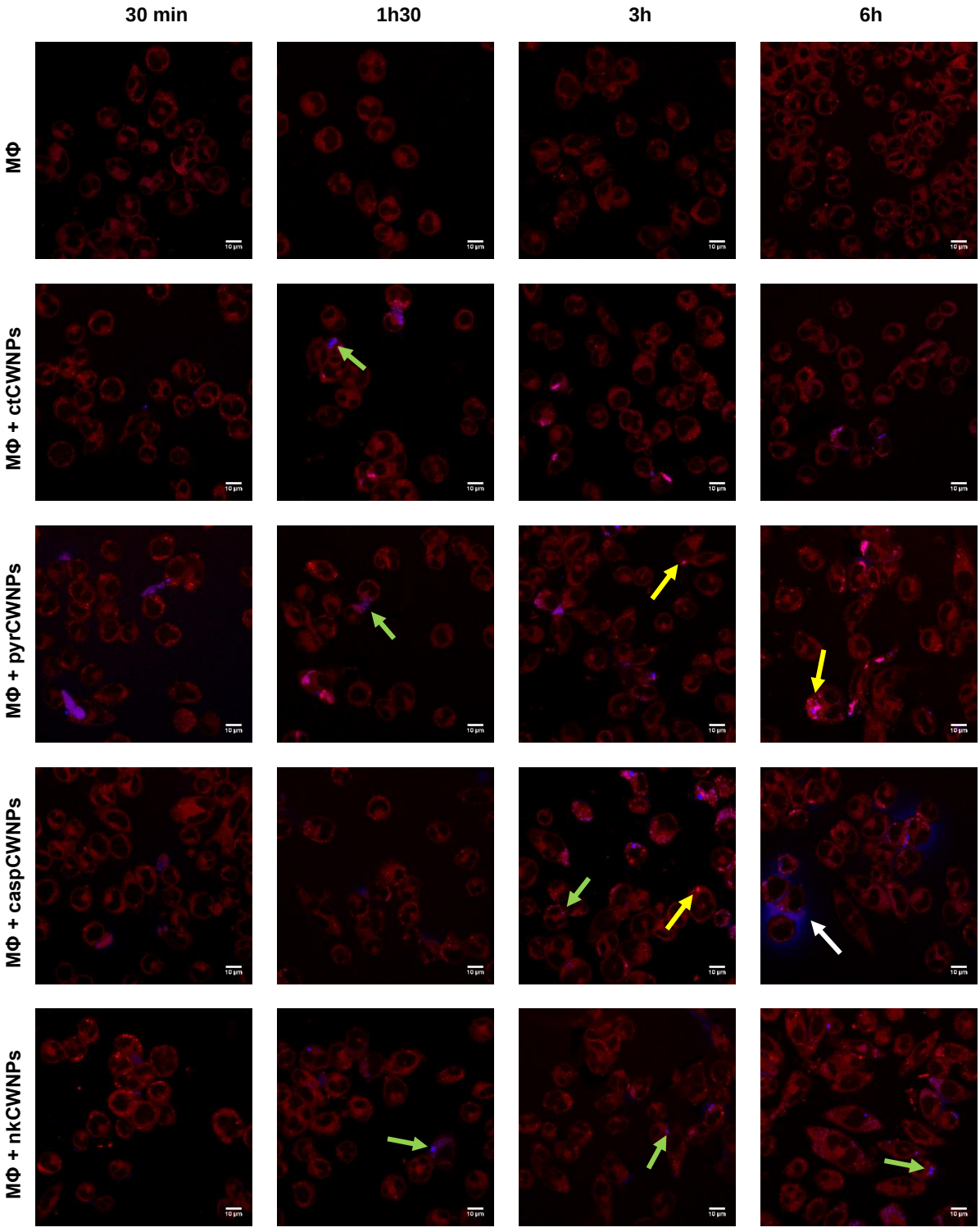

Figure 11: Intracellular distribution of CWNPs *A. infectoria* in RAW 264.7 macrophages and acidic compartments. Macrophages were exposed during 0.5, 1.5, 3 and 6 h to CWNPs of *A. infectoria (*ctCWNPs) and *A. infectoria* grown with 50 µg/mL pyroquilon (MΦ+pyrCWNPs), with 1 µg/mL caspofungin (MΦ+casCWNPs) or with 0.5 µg/mL nikkomycin (MΦ+nkCWNPs) , with ratio 1:1. The NPs were labelled with CFW (Flurescent Brightener 28, Sigma®), a probe for fungal cell wall chitin, and macrophage cytoplasm was labelled with LysoTracker Red® (Red DND-99, Invitrogen), a fluorescent probes that responds to acidic

intracellular compartments. White arrows represent a blue halo around the macrophage; yellow arrows brighter acidified red points; green arrows blue points not overlapped with red fluorescence. Molecular Probes®). Scale bar indicates 10 µm. The cell imaging was performed on a Carl Zeiss LSM 710 Confocal Microscope, using a 63x PlanApoChromat (NA 1.4) oil objective.

To proceed further on in the characterisation of the macrophages activation, during the interaction with the different CWNPs, fluorescent assays was undertaken. With this it was meant to observe the intracellular localization of CWNPs, to quantify the number of CWNPs internalized, the average of nanoparticles' area and to study the intracellular acidification due to macrophage activation by CWNPs stimulation.

The acidified compartments were labelled with Lysotracker Red® (red), a widely used probe to observe the acidification of phagolysosomes. Before the interaction, the CWNPs were labelled with CFW (blue), that binds chitin in the CWNPs.

The results showed that RAW 264.7 mouse macrophages not stimulated by CWNPs contact had the typical morphology and acidified compartments distribution at the four time points (Figure 11).

In what regards morphology, the macrophages interacting with the ctCWNPs did not change morphology during the 6 h interaction. However, macrophages exposed to pyrCWNPs, after 3 h, adopt different irregular forms and some of them became bigger; these changes are more evident at 6 h interaction; the same was observed in the macrophages interacting the nkCWNPs. The caspCWNPs, lead to macrophages morphological changes since 1 h 30 min interaction.

In what concerns the labelling with Lysotraker Red®, i.e., probing for acidic compartments in the macrophages, as a measure of macrophage activation, it revealed that pyrCWNPs trigger an increase in phagolysosome activation, since the macrophages have brighter red fluorescence beginning at 3 h interaction. More, the macrophages interacting with caspCWNPs has bright red points since the 30 min incubation, however this last condition in study (MΦ+nkCWNPs) does not shows homogeneous brighter red fluorescence during the four time points in study.

The blue label of the nanoparticles shows that the nanoparticles were internalized. Surprisingly, caspCWNPs lead to the development, at the 6 h-interaction period, of a blue halo (white arrow, Figure 11) around the macrophages. Another result observed using this strategy is that the blue labelling of the CWNPs is not always overlapped (green arrown, Figure 11) with red fluorescence of the acidified compartments corresponding to phagolysosomes.

3.2.5.1. Characterization of the dynamics of CWNPs when interacting with macrophages

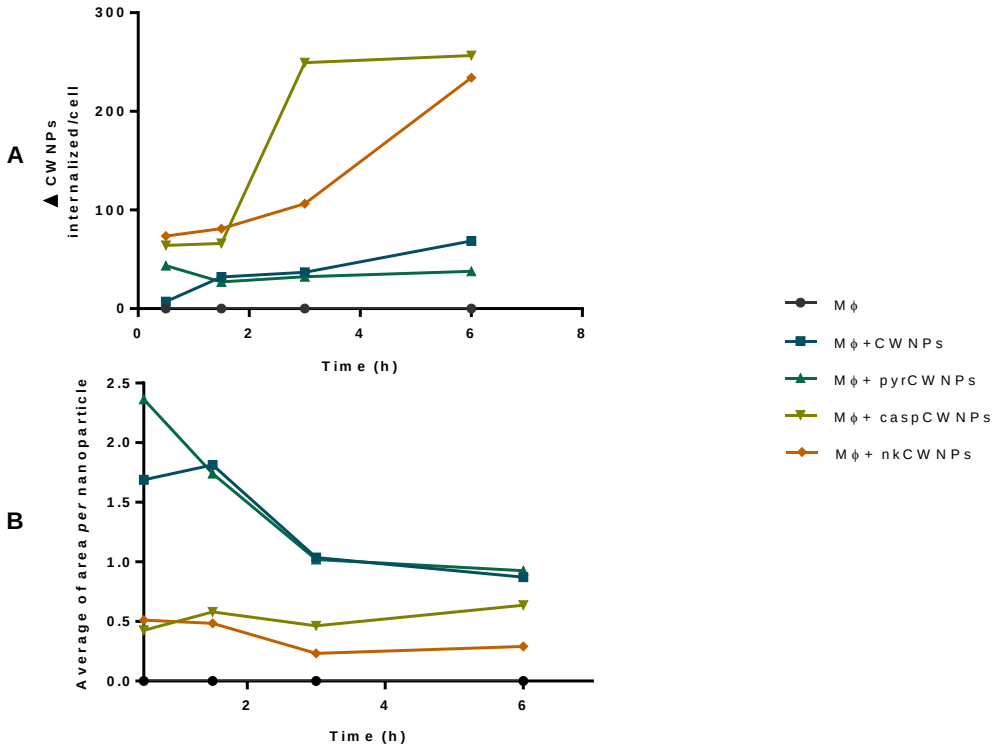

Figure 12: Analysis of area and number of CWNPs internalized by RAW 264.7. Macrophages were exposed during 0.5, 1.5, 3 and 6 h to CWNPs of *A. infectoria* (ctCWNPs) and *A. infectoria* grown with 50 µg/mL pyroquilon (MΦ+pyrCWNPs), with 1 µg/mL caspofungin (MΦ+casCWNPs) or with 0.5 µg/mL nikkomycin (MΦ+nkCWNPs), with ratio 1:1. A) Represents variation of the number of ctCWNPs, pyrCWNPs, caspCWNPs and nkCWNPs internalized during the interaction with the macrophages RAW 264.7. B) Represents the variation of the average area of each particle. This counting was made through Fiji using ImajeJ Plugging Cell Counter using at least 5 images for each condition at each time point of the interaction; Threshold at 50. Results are the mean of each counting.

Taking advantage of software Fiji with ImageJ Plugging Cell Counter, it was possible to analyse other important parameters relating the variation of CWNPs' number internalized by macrophages during the 6 h interactions assay (Figure 12A).

The ctCWNPs and pyrCWNPs, had a similar internalization pattern. Otherwise, the internalization of caspCWNPs or with nkCWNPs, increases constantly after 3h interaction with the macrophages. However, the increase of nkCWNPs it is not as steep as the number of caspCWNPs, which from 3 h to 6 h hours interaction kept the same number of internalized nanoparticles.

Another parameter quantified using Fiji with ImageJ Plugging Cell Counter software was the change on CWNPs' size during the interaction with the macrophages (Figure 12B). This size variation may be cause by particles aggregation (bigger particles)

or by degradation of the particles by macrophages' mechanisms of eliminating pathogens (smaller particles).

During the interaction with the macrophages, the pyrCWNPs show a steeper decrease on their area, similar to the decrease of the ctCWNPs. Furthermore, the area of the caspCWNPs or nkCWNPs kept constant during 6 h-period assay, except for a slight decrease of nkCWNPs (Figure 12B).

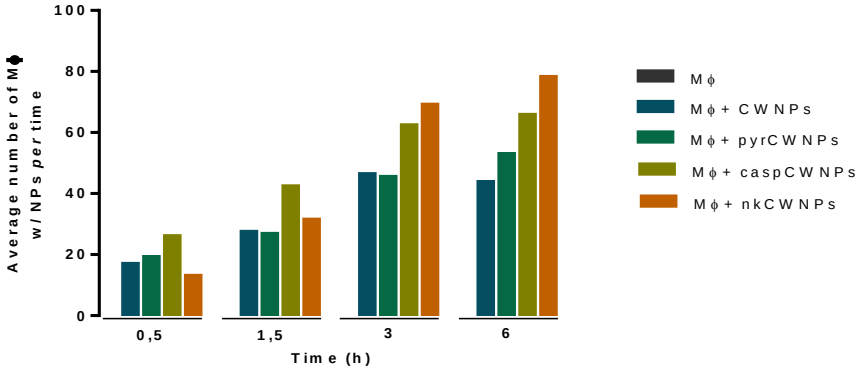

Figure 13: Average number of macrophages that internalized CWNPs *per* time. Macrophages were exposed during 0.5, 1.5, 3 and 6 h to CWNPs of *A. infectoria* (ctCWNPs) and *A. infectoria* grown with 50 µg/mL pyroquilon (MΦ+pyrCWNPs), with 1 µg/mL caspofungin (MΦ+casCWNPs) or with 0.5 µg/mL nikkomycin (MΦ+nkCWNPs), with ratio 1:1. This counting was made through Fiji using ImajeJ Plugging Cell Counter using at least 5 images for each condition at each time point of the interaction, the count was normalized for the total number of cell in each image; Threshold at 50. Results are the mean of each counting

To characterize the model of interaction of CWNPs with the macrophages it is important to evaluate the average number of macrophages that internalized CWNPs. For that, it was counted the number of cells that internalized CWNPs and this number was normalized with the total cell number on each image.

Therefore, we observed the number of macrophages containing CWNPs increases constantly through the duration of the assay with, apparently, a delayed internalization of the nkCWNPs.

3.2.5.2. 3D analysis

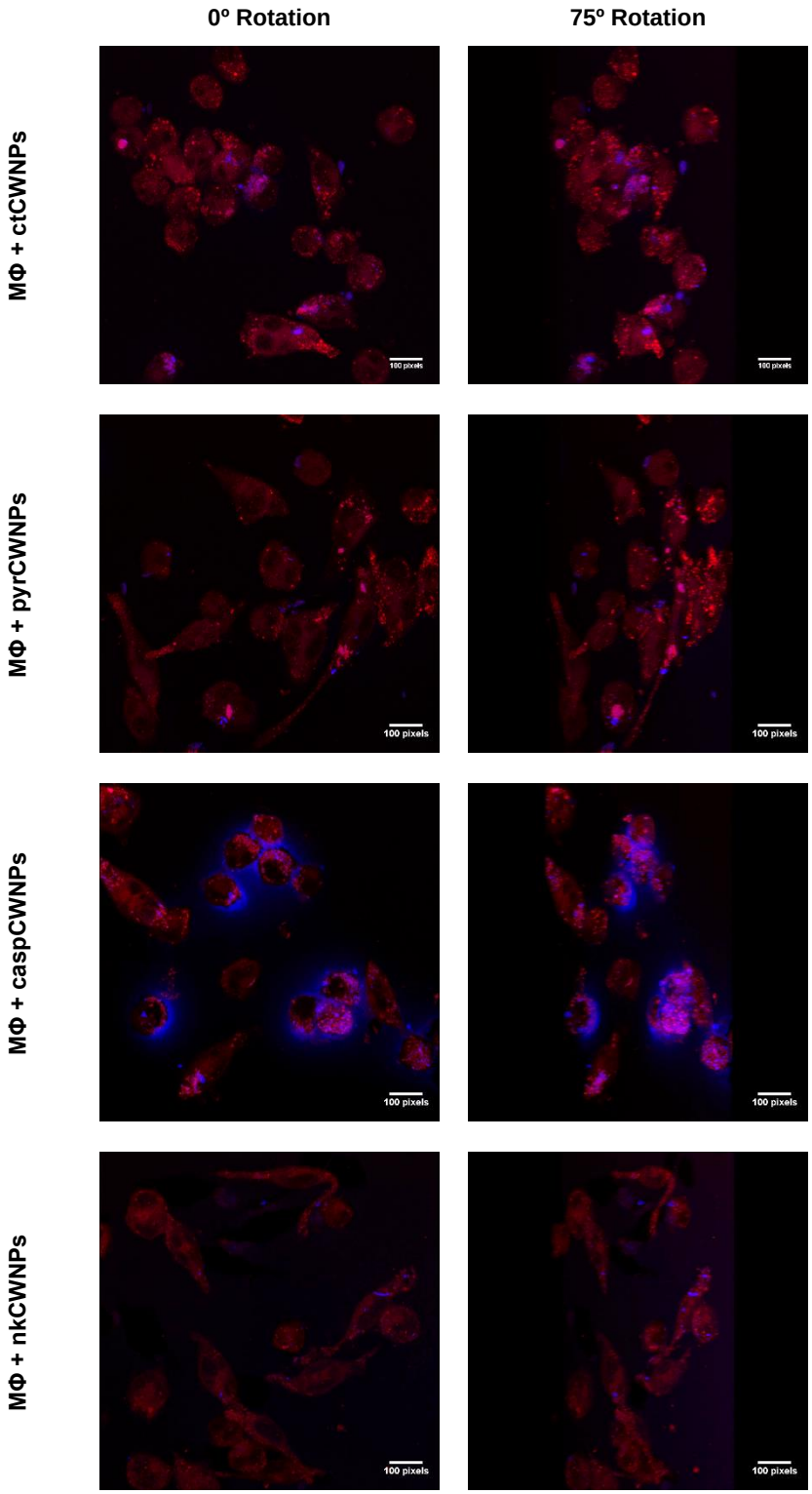

Figure 14: 3D projections of *A. infectoria* CWNPs, in RAW 264.7 macrophages. Macrophages were exposed during 3 h to CWNPs of *A. infectoria* (ctCWNPs) and *A. infectoria* grown with 50 µg/mL pyroquilon (MΦ+pyrCWNPs), with 1 µg/mL caspofungin (MΦ+casCWNPs) or with 0.5 µg/mL nikkomycin (MΦ+nkCWNPs), with ratio 1:1. The CWNPs were labelled with CFW (Flurescent Brightener 28, Sigma®), a probe for fungal cell wall chitin, and macrophage was labelled with LysoTracker Red® (Red DND-99, Invitrogen), a fluorescent probes that responds to acidic intracellular compartments. Molecular Probes®).Scale bar indicates 100 pixels. The cell imaging was performed on a Carl Zeiss LSM 710 Confocal Microscope, using a 63x PlanApoChromat (NA 1.4) oil objective and Z-stack experiment.

In view of determining the CWNPs localization inside the macrophages, we proceed with 3D projection of the images captures by fluorescent microscopy. The confocal laser scanning microscope allows the optical sectioning in the Z axis, capturing a series (stacks) of images focused at regularly placed intervals allowing the visualization of the image in 3D.

This way, we can observe the CWNPS internalized, within these we found some overlapped with the red fluorescent dots (phagolysosomes), presenting a pink colour; other are localize randomly in the cell (not overlapped with the red fluorescent dots).

However, in all conditions we can see some CWNPs out of the macrophage limit, suggesting that these CWNPs may be grabbed to the cell. Furthermore, on the condition with the caspCWNPs we observe a halo around the cell.

3.2.6. Relative quantification of Tumor necrosis factor alpha gene (TNF-α) expression in macrophages during interaction with CWNPs

Tumor necrosis factor alpha (TNF-α) is a proinflammatory cytokine released by several cell types, such as macrophages. Once is a proinflammatory cytokine necessary for the development of effective innate and adaptive immunity to fungal infections, it was relevant to study if the expression of TNF-alpha gene is altered by the presence of the different CWNPs.

The quantitative real time RT-PCR (qPCR) showed that in a population of macrophages interacting with ctCWNPs, the expression of the TNF-alpha gene did have a meaningful change, as proved by the relative amounts of specific RNA (Figure 12) on the two-time points studied. Among all the other assays where macrophages were exposed to CWNPs prepared from *A. infectoria* grown with several inhibitors of cell wall components only the caspCWNPs lead to a significant increase in the expression of the gene coding for the cytokine TNF-α. Most of the date gathered was obtained from samples taken after 3 h interaction between macrophages and CWNPs.

Nevertheless, a preliminary study was performed with samples taken at 1 h-interaction and it indicates and proves that the response is negative for all conditions, except for caspCWNPs in which the activation of gene expression, quantified by the relative amount of specific mRNA, is even higher than at the 3 h-interaction period.

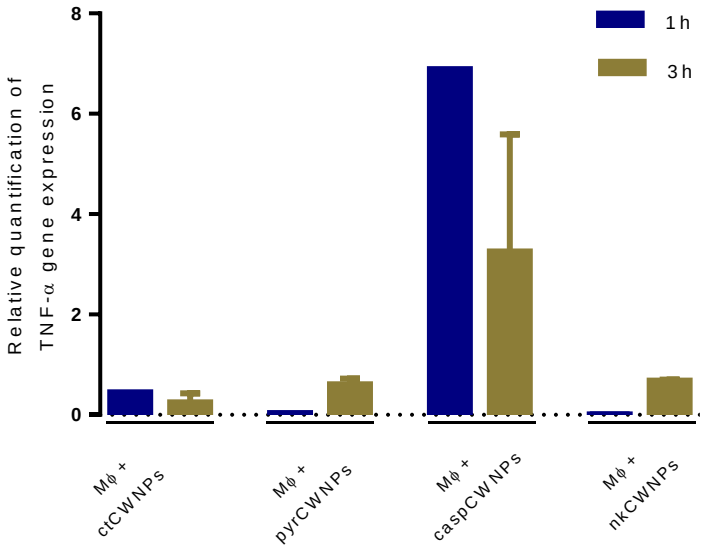

Figure 15: Relative quantification of Tumor necrosis factor alpha gene (TNF-α) expression in macrophages after 1 h and 3 h interaction with ctCWNPs and growth fungi of CWNPs with 50 µg/mL pyroquilon (pyrCWNPs), 1 µg/mL caspofungin (caspCWNPs) and 0,5 µg/mL nikkomycin (nkCWNPs). The relative quantification of TNF-alpha gene was analysed through the dissociation curve obtained from the PCR reaction, which used the EvaGreen dye (fluorescent nucleic acid dye). The maximum peak of the curve occurs at 86 ºC and correspond to a single amplicon. The GAPDH gene was used as reference. The data was analysed by relative quantification using the $2^{-\Delta\Delta Ct}$ method for each gene using the Ct values (Schmittgen & Livak, 2008). b) Relative quantification of TNF-α gene expression in CWNPs and pyrCWNPs, caspCWNPs, nkCWNPs interaction with macrophages in two different time points. The results are presented as mean ± SEM, with n=3 for the time of 3 h interaction and means for 1 h interaction, with n=1.

Chapter 4

Discussion

4. Discussion

Fungal diseases represent a growing threat, mostly caused by the increase of immunocompromised individuals, namely under cytotoxic anti-cancer therapies, chemotherapy, organ transplantation, autoimmune diseases and AIDS (Romani, 2011). The diseases caused by fungi are very likely associated with the interaction of components of the cell wall with the host cells. The fungal cell wall is a dynamic structure, continuously evolving in response to the environment and during growth. Additionally, it has been recognized the importance of fungi in the onset of severe respiratory diseases, due to fungal sensitization, in people exposed to fungal particles, spores or parts of mycelial hyphae (Denning *et al*., 2014). *A. infectoria* is a human pathogen, identified as one of the most common airborne fungal particles, triggering the research interest of how this opportunistic pathogen can cause disease (Murai *et al.*, 2012).

The main goal of this research was to construct a new model of interaction between macrophages and filamentous fungi that would allow us the study of the immunomodulatory effect of certain components of the fungal cell wall. For that we used *A. infectoria* cell wall to prepare nanoparticles with different content on chitin, β-glucan and melanin (DHN-melanin) and proceeded to interaction assays with a mouse macrophages cell line, RAW 264.7.

4.1 Nanoparticles characterization

Filamentous fungi are difficult to study in what regards its ability to interact, *in vitro*, with phagocytic cells since the germination of spores and the hypha evoke a strong response from those cells, rapidly conducting to host cell death. Therefore, it emerged the need of creating a new model to study all the mechanisms existing on interaction between the host immune system and the fungi. This way, the first part of this work rely on the preparation and characterization of nanoparticles prepared from the cell wall of *A. infectoria* (CWNPs). To study different components of the fungal cell wall, we prepared the CWNPs from *A. infectoria* grown with different compounds, that modulate the cell wall content in chitin, β-(1,3)-glucan and melanin.

One of the compounds that the fungi grew with, was caspofungin. The first echinocandin used in human health, targeting the β-(1,3)-glucan synthase (Kartsonis *et al*., 2003). *A. infectoria* mycelia grown in the presence of caspofungin (caspCWNPs) leads to a darker mycelia than when grown under control conditions, which is an evidence of higher melanin content, as described by our research group (Fernandes *et al*., 2016), decreases the β-(1,3)-glucan and keep the content in chitin unchanged. Another component in study is an inhibitor of DHN-melanin synthesis, pyroquilon, with

which it was observed a lighter colour on *A. infectoria* mycelia, due to the decrease of DHN-melanin synthesis. Nikkomycin Z, a chitin synthase inhibitor, was used to modulate the chitin of cell wall of *A. infectoria*. As reported by Fernandes *et al*. (2014), with this compound the content in melanin increases, causing darker coloured mycelia, almost black and it increases the content in chitin. This last result, apparently paradoxal, since the fungus was grown with a chitin synthase inhibitor, was described before (Fernandes *et al*., 2016) and rely on the existence of eight different chitin synthases isoforms, which overactivation leads to increase in the chitin cell wall content (Fernandes *et al*., 2014).

CWNPs were prepared from fungal cell walls modulated as described above. A crucial part of this work, was to characterize the obtained CWNPs to know the differences between them depending on the condition of fungi growth, from which the CWNPs were prepared and, ultimately, predict their behaviour on the interaction assays with the macrophages.

All the CWNPs had the same morphology, spherical, thereby the metric particle diameter is enough to descript the particle size (Hassellöv *et al*., 2008). The size analysis showed that nanoparticles from *A. infectoria* grown with pyroquilon and caspofungin (pyrCWNPs and caspCWNPs), were smaller than the fungi grown under control condition.

The potential zeta of the NPs is another parameter to have in count on CWNPs characterization. Potential zeta determines surface charge of the particles and closely relates to suspension stability and particle surface morphology. The mobility is converted in zeta potential through Smoluchowsky's theory (Hassellöv *et al*., 2008). Therefore, the potential zeta value of pyrCWNPs, caspCWNPs and nkCWNPs are meaningful lower than the CWNPs of fungi grown under control condition (ctCWNPs). However, all the values are higher than -25 mV and lower than 25 mV, which means the nanoparticles does not have a strong force repelling one another (Tantra *et al*., 2010), consequently the CWNPs have a disposition to form aggregates.

The potential zeta values may be due to the differences on the charge of the CWNPs surface. Since the melanin pigment is negatively charged, the pyrCWNPs, probably will have less negative ions, turning the surface of the nanoparticle more positive, while the chitin is strongly positive and β-(1,3)-glucan is a zwitterionic polysaccharide (electrically neutral). So, it is expected that, caspCWNPs had more negative surface (equal chitin content, less β-(1,3)-glucan and more melanin content) while the nkCWNPs (more chitin and melanin content and equal glucan) have an electrical neutral surface. The tendency to form aggregates provokes an over-evaluation of the measured sizes of the CWNPs obtained with DLS. However, on TEM technique was possible to measure the size of one particle only.

One of the limitations of this study was that, it was not possible to quantify the CWNPs content in chitin, β-(1,3)-glucan and melanin, after its preparation, to confirm if the relative content of each component did not suffered changes during the mechanical process. This limitation was due to the techniques currently used in the lab to quantify these components; to achieve this it should be implemented an immune quantitative assay.

4.2 Macrophages-CWNPs interaction characterization

The surveillance and elimination of fungal pathogens rely heavily on the sentinel behaviour of phagocytic cells, such as macrophages. To the fungi, the cell wall is the first point of contact playing an important role in the recognition and phagocytosis by the immune cells (Latgé, 2015). However, most of what is known about fungal-host interaction is derived from *C. albicans* and from *Aspergillus fumigatus* studies, and a lack of knowledge exists in what concerns how the different filamentous fungi cell wall components interact with the host cells. Having this in view, different CWNPs were prepared from fungal cell walls obtained from mycelia grown in the presence of cell wall inhibitors and observed the macrophages response to those CWNPs.

To characterize the immune response of the macrophages interaction with the different CWNPs, it was evaluated, during the interaction, the macrophages viability, morphology and cytokine response; it was observed the aggregation or degradation of CWNPs, intracellular location and dynamics. A trypan blue assay was used to identify the macrophages viability (Freshney, 1994). Microscopy assays were accomplished labelling sialic acids and acids deoxyribonucleic, or acidified compartments and CWNPs' chitin. The sialic acids are a family of sugars found attached to glycans on the cell surface (Lin et al., 2010; Varki & Gagneux, 2012), and were used to delimit the macrophages membrane, while DAPI is known to form complexes with natural double-stranded DNA. The other fluorescent probe used were LysoTracker Red®, to label the acidified compartments inside macrophages and CFW, that binds to β-(1,3) and β-(1,4) polysaccharides, such as chitin (Harrington *et al*., 2003), present on the CWNPs.

The nanoparticles from *A. infectoria* cell wall grown in the absence of cell wall components inhibition (ctCWNPs) evoke a macrophages response similar to that observed with live conidia (Cruz-Almeida, 2013), with the macrophages keeping their morphology and retaining viability during the interaction assay.

The detailed study of the internalization between the macrophages and ctCWNPs by TEM revealed that the internalization of the CWNPs occurs through a process of phagocytosis, with the engulfment of the particles through a membranous compartment,

the phagosome. Once internalized, the phagosome suffers maturation with the fusion of lysosomes, leading to progressive acidification and acquisition of enzymes and oxidants (Erwig & Gow, 2016). However, some CWNPs are found free in the macrophages cytoplasm. This result can be interpreted as the release of the CWNPs from the phagosome, before its maturation, as demonstrated using fluorescent probes that indicates an absence of the acidification of the compartments containing ctCWNPs.

To modulate the content of β-(1,3)-glucan in *A. infectoria* cell wall, the fungus was grown with caspofungin. Caspofungin inhibits the synthesis of β-(1,3)-glucan, and increases the melanin content (Fernandes *et al.*, 2014; *Fernandes et al*., 2016). The cell wall nanoparticles of *A. infectoria* grown with caspofungin (caspCWNPs) trigger a macrophages response different than ctCWNPs.

In fact, in the presence of caspCWNPs the macrophages viability decreased and there was a change in the morphology (enlarged and stretched). The results suggest that although caspofungin alters the β-(1,3)-glucan inhibiting its synthesis, the remaining few is probably more exposed (Wheeler & Fink, 2017). Since β-(1,3)-glucan is known to have a strong immunostimulatory effect (Seider *et al*., 2010), this would justify a higher triggering of the macrophages activation.

During the interaction, there was an increase of acidified compartments on macrophages. The most surprising result observed with the fluorescence microscopy during the interaction of macrophages with caspCWNPs it was the occurrence of a blue halo (due to the label of chitin with CFW) around the delimitated macrophage membrane. This result suggests that the caspCWNPs lead to a higher recruitment of lysosomes to phagosomes, and its maturation into phagolysosomes (increase acidified compartments) to “kill” the “pathogen”. We believe that, enzymes release and activated inside the phagolysosomes, disaggregate and pursue the degradation of the caspCWNPs into their building block (smaller molecules), that were released to the extracellular milieu. This was also proved by the observed decrease of caspCWNPs area, with the increase of its internalization. It is known that macrophages, in response to microorganisms produce several degradating enzymes, including glycosidases that can hydrolyse chitin (Weiss & Schalb, 2015). The release of the degradation products of the caspCWNPs by the macrophage might function as a messenger of a fungal “infection” to other immune cell (Nimrichter *et al.*, 2016).

Nanoparticles were prepared from *A. infectoria* grown with nikkomycin (nkCWNPs), to modulate their content in chitin, and compared with the macrophages response interaction with ctCWNPs, caspCWNPs and pyrCWNPs. The results showed

that nkCWNPs caused a delayed macrophage response and also a delay of their internalization.

TNF-α is one of the central signalling molecules produced in inflammatory response. Only macrophages interacting with caspCWNPs show a significant increase in expression of TNF-alpha gene. Although the cytokine was not quantified, TNF-α is induced by activation of Dectin-1 (Esteban *et al*., 2011), which it is activated by β-(1,3)-glucan (Douwes, 2005). On caspCWNPs, the β-(1,3)-glucan are more exposed while on nkCWNPs and pyrCWNPs may have that component not so exposed or masked with the melanin or with the chitin content.

The macrophages viability decreased and morphology change to enlarged and stretched cells, a typical morphology of activated macrophages. This result can be related to, as stated before, to nikkomycin increasing the chitin content but also leading to different chitin organization; these events are also linked to changes in the pattern of melanin deposition: increased content (Fernandes *et al*., 2016) and in the pattern of deposition (Walker *et al.*, 2010). Another important aspect is that chitin tend to be immunosuppressive by blocking dectin-1 mediated engagement (Netea *et al*., 2011). Also, melanin has been reported the possibility of masking the immunomodulatory components of cell wall (Nosanchuck & Casadevall, 2006).

Overall, these results suggest that the macrophage activation by nkCWNPs did not occur during the internalization step but only after phagocytosis, when the nkCWNPs where already inside the phagosome, during the nanoparticles degradation into their building blocks.

Pyroquilon was used to modulate the DHN-melanin content on *A. infectoria* cell wall, the only melanin present in this filamentous fungus (Fernandes *et al*., 2016). The cell wall nanoparticles of *A. infectoria* grown with pyroquilon (pyrCWNPs) caused a higher macrophage activation when compared with the macrophages response to ctCWNPs. The macrophages showed irregular forms (more enlarged and stretched) and a decreased viability. Although the organization of the cell wall components in the CWNPs prepared was not studied in detail, these results suggest an effect similar to those describing that the inhibition of the synthesis of the outer layer of melanin of the fungal cell wall provides the exposure of the inner layers with components that trigger a macrophages stimulation, i.e. β-(1,3)-glucan (Nosanchuck & Casadevall, 2006). This way, melanin may have an important role on recognition of *A. infectoria*. Also, with the inhibition of melanin it was verified an increase of acidified compartments, suggesting that melanin, when present, may be responsible for the inhibition of the acidification of phagosomes (Thywißen *et al*., 2011), interfering with maturation.

Furthermore, the internalization pattern of pyrCWNPs was similar to the internalization pattern of ctCWNPs when interacting with macrophages, suggesting that melanin does not interfere in the fungi internalization, but mainly in the macrophages recognition and activation. In addition, the area of the nanoparticles also decreases with a similar pattern of the ctCWNPs, which may be due only to the CWNPs disaggregation when in the phagolysosomes.

Chapter 5

Final Conclusions

5. Final Conclusions

Fungal infections are a life-threatening and emergent disease, mainly because of the increase of the immunocompromised population and of allergic diseases due to airborne fungal particles, as spores or hyphal particles. The main goals of this work were to develop a new model of interaction between filamentous fungi and macrophages using fungal cell wall nanoparticles, and the immunomodulatory effect of components of *A. infectoria* cell wall. The cell wall components levels were modulated using inhibitors: caspofungin, an inhibitor of β-(1,3)-glucan synthesis; nikkomycin Z, an inhibitor of chitin synthases; pyroquilon, an inhibitor of DHN-melanin synthesis.

The conclusion to de drawn out of this work are as follows:

- The nanoparticles prepared out of fungal cell walls obtained with the different grown conditions, independent on their different content in β-(1,3)-glucan, chitin and DHN-melanin, are spherical with average siz ranging from 70.19 to 365.2 nm and tend to aggregate.
- The most important results achieved with this work is that the CWNPs are a good model to study the interaction between macrophages and filamentous fungi
    - The interaction of ctCWNPs showed that the nanoparticles are internalized by phagocytosis, and after this internalization by the macrophages they may be both located in phagolysosomes or free in the cytoplasm.
    - As observed before with the live conidia of *A. infectoria*, ctCWNPs do not evoke a response in macrophages.
    - The caspCWNPs, with a low level of β-(1,3)-glucan but more exposed to the recognition by host cells receptors, trigger a high macrophage activation, namely with a 6-fold (1 h exposure) or 3-fold (3 h exposure) increase of TNF-alpha gene expression.
    - Through the inhibition of DHN-melanin, the pyrCWNPs trigger macrophage activation, showing the crucial role of melanin on *A. infectoria* recognition, namely the DHN-melanin role on masking the fungal cell wall components.
    - The increased of chitin and melanin in nkCWNPs, caused a delayed macrophage activation, proving the immunossupressive effect of these cell wall components.

Chapter 6

Future Perspectives

6. Future Perspectives

This research work represents a pleasing addition to improve the study of mechanisms of recognition and interaction of the cell wall of filamentous fungi with macrophages.

However, it remains to be elucidated some aspects:

- The TNF-α gene expression by macrophages should be done in another (earlier) time point of the interaction with the CWNPs, and protein quantification is also needed;
- The β-(1,3)-glucan and chitin content quantification of the cell wall of *A. infectoria* grown with pyroquilon
- To clarify if the content in melanin, β-(1,3)-glucan and chitin after the CWNPs preparation remains the same as before the preparation

A future research objective to follow this work is to use the CWNPs characterized in this work to comprehend not only the innate immune system response, *in vitro*, but the immune response in a whole, *in vivo*. This way, we would understand the mechanisms underlying invasive diseases and fungal sensitization, using mices to be sensitized to fungi by intranasal instillation (Ghosh *et al*., 2014).

Chapter 7

Bibliographic references

7. Bibliographic References

Andersen B. T. U. (1996) “Differentiation of *Alternaria infectoria* and *Alternaria alternata* based on morphology, metabolite profiles, and cultural characteristics.” Can J Microbiol. 1996;**42**(7):685-689.

Anjos J., Fernandes C., Silva B. M. A., Quintas C., Abrunheiro A., Gow N. A. R., Gonçalves T. (2012) “β-(1,3)-glucan synthase complex from *Alternaria infectoria*, a rare dematiaceous human pathogen.” Med Mycol. **50**(7):716-725.

Brand A. (2012) “Hyphal Growth in Human Fungal Pathogens and Its Role in Virulence.” Int J Microbiol **2012**:517529.

Casadevall, A., Nosanchuk J. D., Williamson P. and Rodrigues M. L. (2009). "Vesicular transport across the fungal cell wall." Trends in Microbiology **17**(4): 158-162.

Cruz-Almeida, M. L. (2013) “Characterization of innate immune response to *Alternaria infectoria*” (Master thesis) FCTUC Ciências da Vida – Teses de Mestrado.

Da Silva C. A., Chalouni C., Williams A., Hartl D., Lee C .G., Elias J.A. (2009) “Chitin Is a Size-Dependent Regulator of Macrophage TNF and IL-10 Production.” J Immunol. **182**(6):3573-3582.

Denning D. W., Pashley C., Hartl D., Wardlaw A., Godet C., Giacco S. D., Delhaes L., Sergejeva S. (2014) Fungal allergy in asthma–state of the art and research needs. Clin Transl Allergy.**4**(1):14.

Douwes J. (2005) “(1 → 3)-β-D-glucans and respiratory health : a review of the scientific evidence.” Indoor Air **15**:160-169.

Eduard W. (2009) “Fungal Spores: A Critical Review of the Toxicological and Epidemiological Evidence as a Basis for Occupational Exposure Limit Setting” Critical Reviews in Toxicology **39** (10): 799–864.

Eisenman H. C., Casadevall A. (2012) “Synthesis and assembly of fungal melanin.” Appl Microbiol Biotechnol. **93**(3):931-940.

Enjalbert B., Smith D. A., Cornell M. J., Alam I., Nicholls S., Brown A. J., Quinn J. (2006) "Role of the Hog1 stress-activated protein kinase in the global transcriptional response to stress in the fungal pathogen *Candida albicans*." Mol Biol Cell. **17**(2):1018-1032.

Erwig L. P., Gow N. A. R. (2016) "Interactions of fungal pathogens with phagocytes." Nature Reviews Microbiology **14**:163-176.

Esteban A., Popp M. W., Vyas V. K., Strijbis K., Ploegh H. L., Fink G. R. (2011) "Fungal recognition is mediated by the association of dectin-1 and galectin-3 in macrophages." PNAS **108**(34):14270-14275.

Fernandes C., Anjos J., Walker L. A., Silva B. M. A., Cortes L., Mota M., Munro S. A., Gow N. A. R., Gonçalves T., (2014) "Modulation of *Alternaria infectoria* cell wall chitin and glucan synthesis by cell wall synthase inhibitors." Antimicrob Agents Chemother. **58**(5):2894-2904.

Fernandes C., Gow N. A. R., Gonçalves T. (2016) "The importance of subclasses of chitin synthase enzymes with myosin-like domains for the fitness of fungi." Fungal Biology Reviews **30**:1-14

Fernandes C., Prados-Rosales R., Silva B., Nakouzi-Naranjo A., Zuzarte M., Chatterjee S., Stark R. E., Casadevall A., Gonçalves T. (2016) "Activation of melanin synthesis in *Alternaria infectoria* by antifungal drugs." Antimicrob Agents Chemother. **60**(3):1646-1655.

Ferrer, C., J. Montero, J. L. Alio, J. L. Abad, J. M. Ruiz-Moreno and F. Colom (2003). "Rapid Molecular Diagnosis of Posttraumatic Keratitis and Endophthalmitis Caused by *Alternaria infectoria*." Journal of Clinical Microbiology **41**(7): 3358-3360.

François J. M. (2006) "A simple method for quantitative determination of polysaccharides in fungal cell walls." Nat Protoc. **1**(6):2995-3000.

Freshney J. (1994) "Animal Cell Culture: Introduction to Biotechniques" *Bioessays* 16:218-218.

Giraldo M. C., Valent B. (2013) "Filamentous plant pathogen effectors in action." Nat Rev Microbiol. **11**(11):800-814.

Ghosh S., Howe N., Volk K., Tati S., Nickerson K. W., Petro T. M. (2010) "*Candida albicans* cell wall components and farnesol stimulate the expression of both inflammatory and regulatory cytokines in the murine RAW264.7 macrophage cell line" FEMS Immunol Med Microbiol **60**:63-73.

Ghosh S., Hoselton S.A., Asbach S. V., Steffan B. N., Wanjara S. B., Dorsam G. P., Schuh J. M. (2015) "B lymphocytes regulate airway granulocytic inflammation and cytokine production in a murine model of fungal allergic asthma." Cell Mol Immunol. **12**(2):202-212.

Harrington B. J., Hageage G. J. (2003) "Calcofluor White: A Review of its Uses and Applications in Clinical Mycology and Parasitology" Your Lab Focus **34**(5).

Hassellöv M., Readmen J. W., Ranville J. F., Tiede K. (2008) "Nanoparticles analysis and characterization methodologies in environmental risk assessment of engineered nanoparticles" Ecotoxicology **17**:344-361.

Hipolito E., Faria E., Alves A. F., Hoog G. S., Anjos J., Gonçalves T., Morais P. V., Estevão H., (2009) "*Alternaria infectoria* brain abscess in a child with chronic granulomatous disease." Eur J Clin Microbiol Infect Dis. **28**(4):377-380.

Hwang, C. S., Flaishman M. A., and Kolattukudy P. E. (1995). "Cloning of a Gene Expressed during Appressorium Formation by *Colletotrichum gloeosporioides* and a Marked Decrease in Virulence by Disruption of This Gene." The Plant Cell. **7**:183-193.

Jacobson, E. S. (2000). "Pathogenic roles for fungal melanins." Clinical Microbiology Reviews **13**: 708-717.

Kartsonis N.A., Nielsen J., Douglas C.M. (2003) "Caspofungin: the first in a new class of antifungal agents." Drug Resist Updat. **6**(4):197-218.

Kong L. A., Yang J., Li G. T., Qi L. L., Zhang Y. J., Wang C. F., Zhao W. S., Xu J. R., Peng Y. L., (2012) "Different chitin synthase genes are required for various developmental and plant infections processes in the rice blast fungus *Magnaporthe oryzae.* PLoS Pathog **8**: e1002526.

Langfelder K., Streibel M., Jahn B., Haase G., Brakhage A. A. (2003) “Biosynthesis of fungal melanins and their importance for human pathogenic fungi.” Fungal Genet Biol. **38**(2):143-158.

Larone, D. H. (2002). Medically important fungi: a guide to identification. Washington, D.C.

Latgé, J.P. (2007). "The cell wall: a carbohydrate armour for the fungal cell." Molecular Microbiology **66**(2): 279-290.

Latgé J. P. (2010) “Tasting the fungal cell wall.” Cell Microbiol. **12**(7):863-872.

Latgé J. (2015) “Fungal immunology: from simple to very complex concepts.” Semin Immunopathol **37**:81-82.

Latgé J. P., Beauvais A. (2014) “Functional duality of the cell wall.” Curr Opin Microbiol. **20**:111-117.

Lin, J. S., J. H. Huang, L. Y. Hung, S. Y. Wu and B. A. Wu-Hsieh (2010). "Distinct roles of complement receptor 3, Dectin-1, and sialic acids in murine macrophage interaction with Histoplasma yeast." Journal of Leukocyte Biology **88**(1): 95-106.

Lipke, P. N., Ovalle, R. (1998) 2Cell wall architecture in yeast: new structure and new challenges.” J. Bacteriol. **180**, 3735–3740

Murai, H., H. Qi, B. Choudhury, J. Wild, N. Dharajiya, S. Vaidya, A. Kalita, A. Bacsi, D. Corry, A. Kurosky, A. Brasier, I. Boldogh and S. Sur (2012). "*Alternaria*-Induced Realease of IL-18 from Damaged Airway Epithelial Cells: An NF-κB Dependent Mechanism of Th2 Differentiation?" PloS ONE **7**(2): e30280.

Naseem S., Araya E,., Konopka J. B. (2015) “Hyphal growth in *Candida albicans* does not require induction of hyphal-specific gene expression.” Mol Biol Cell. **26**(6):1174-1187.

Netea M. G., Brown G. D., Kullberg B. J., Gow N. A. R.(2008) “An integrated model of the recognition of *Candida albicans* by the innate immune system.” Nat Rev Microbiol. **6**(1):67-78.

Netea M. G., Mora-montes M., Ferwerda G., Lebardon M. D., Brown G. D., Mistry A. R., Kullberg B. J., O'Callaghan C. A., Sheth C. C., Odds F. C., Brown A. J. P., Munro C. A:, Gow N. A. R. (2011) "Recognition and Blocking of Innate Immunity Cells by Candida albicans Chitin" Infection and Immunity **79**(5):1961-1970.

Nimrichter L., Souza M.M., Poeta M. D., Nosanchick J. D., Joffe L., Tavares P. M., Rodrigues M. L. (2016) "Extracellular Vesicle-Associated Transitory Cell Wall Components and Their Impact on the Interaction of Fungi with Host Cells." Frontiers in Microbiology **7**:1-11.

Nosanchuk J. D., Casadevall A. (2006) "Impact of Melanin on Microbial Virulence and Clinical Resistance to Antimicrobial Compounds." Antimicrobial Agents and Chemotherapy **50**(11):3519-3528.

Onishi, J., Meinz, M., Thompson, J., Curotto, J., Dreikorn, S., Rosenbach, M., et al. (2000) "Discovery of novel antifungal (1,3)-beta-D-glucan synthase inhibitors." Antimicrob Agents Chemother **44**: 368–377.

Pastor F. J., Guarro J. (2008) "*Alternaria* infections: Laboratory diagnosis and relevant clinical features." Clin Microbiol Infect. **14**(8):734-746.

Plato A., Hardison S. E., Brown G. D. (2015) "Pattern recognition receptors in antifungal immunity." Semin Immunopathol **37**:97-106.

Pluddemann, A., S. Mukhopadhyay and S. Gordon (2011). "Innate Immunity to Intracellular Pathogens: Macrophage Receptors and Responses to Microbial Entry." Immunological Reviews **240**: 11-24.

Pombeiro-Sponchiado S. R., Sousa G. S., Andrade J. C. R., Lisboa H. F., Gonçalves R. C. R. (2017) "Production of Melanin Pigment by Fungi and Its Biotechnological Applications" Intech Chapter 4.

Riquelme M. (2013) "Tip Growth in Filamentous Fungi: A Road Trip to the Apex." Annu Rev Microbiol. **67**(1):587-609.

Rokern JS. (2007) “Biotechnology: Industrial mycology” Encyclopedia of Life Systems (EOLSS) **6**: 75-97

Romani, L. (2004). "Immunity to fungal infections." Nature Reviews Immunology **4**(1): 1124.

Romani, L. (2011). "Immunity to fungal infections." Nature Reviews Immunology **11**(4): 275-288.

Schmittgen T. D., Livak K. J. (2008) “Analyzing real-time PCR data by the comparative CT method.” Nat Protoc. **3**(6):1101-1108.

Seider K., Heyken A., Luttich A., Miramon P., Hube B. (2010) “Interaction of pathogenic yeasts with phagocytes: survival, persis- tence and escape.” Curr OpinMicrobiol **13**:392–400

Simon-Nobbe B., Denk U., Pöll V., Rid R., Breitenbach M. (2008) “The spectrum of fungal allergy” Int Arch Allergy Immunol **145**(1):58-86.

Tantra R., Schulze P., Quincey P. (2010) “Effect of nanoparticle concentration on zeta-potential measurement results and reproducibility.” Particuology. **8**(3):279-285.

Thywißen A., Heinekamp T., Dahse H. M., Schmaler-Ripcke J., Nietzsche S., Zupfel P. F., Brakhage A. A. (2011) “Conidial dihydroxynaphthalene melanin of the human pathogenic fungus Aspergillus fumigatus interferes with the host endocytosis pathway.” Front Microbiol **2**(96):1-12.

Treitschke S., Doehlemann G., Schuster M., Steinberg G., (2010) “The myosin motor domain of fungal chitin synthase V is dispensable for vesicle motility but required for virulence of the maize pathogen Ustilago maydis.” Plant Cell **22**: 2476-2494.

Van de Veerdonk F. L., Netea M. G., Jansen T. J., Jacobs L., Verschueren I., van der Meer J. W. M., Kullberg B. J., (2008) “Redundant role of TLR9 for anti-*Candida* host defense.” Immunobiology **213**:613-620.

Varki, A. and P. Gagneux (2012). "Multifarious roles of sialic acids in immunity." Annals of the New York Academy of Sciences **1253**(1): 16-36.

Woudenberg J. H. C., Seidl M. F., Groenewald J. Z., de Vries M., Stielow J. B., Thomma B. P. H. J., and Crous P. W. (2015) "*Alternaria* section *Alternaria*: Species, formae speciales or pathotypes?" Stud Mycol. **82**:1-21

Walker C. A., Gómez B. L., Mora.Montes H. M., Mackenzie K. S., Munro C. A., Brown A. J. P., Gow N. A. R., Kibbler C. C., Odds F. C. (2010) "Melanin Externalization in *Candida albicans* Depends on Cell Wall Chitin Structures" Eukaryotic Cell **9**(9):1329-1342.

Weiss G., Schaible U. E. (2015) "Macrophage defense mechanisms against intracellular bacteria" Immunological Reviews **264**:182-203.

Wheeler M.L., Limon J.J., Underhill D.M. (2017) "Immunity to Commensal Fungi: Detente and Disease." Annu. Rev. Pathol. Mech. Dis. **12**:359–85.

Yabuuchi E, Ohyama A. (1972) "Characterization of pyomelanin producing strains of *Pseudomonas aeruginosa*." Int J Syst Bacteriol. **22**(2):53-64.